

Analysis and Design of Wireless Energy Harvesters for Internet of Things and sub-6GHz 5G Applications

Author: [REDACTED]

Supervisor: [REDACTED]

Date: April 2021

[REDACTED]



Abstract

In this report, a wireless energy harvesting (WEH) component known as a filtenna, a microstrip bandpass filter and various antenna arrays will be designed, analysed, and evaluated for use in 5G Internet of Things (IoT) applications. A filtenna is the combination of a filter and an antenna, into a single component that achieves both filtering and radiating functions. The physical dimensions are determined using the relevant calculations described throughout this report and the reflection and transmission loss behaviour of the designed components is simulated and analysed using the Advanced Design System (ADS) software. The results from simulating the initial design will be used to improve upon the design of the filtenna circuit and provide the specified behaviour.

The microstrip patch antenna and antenna arrays will receive RF signals around the 3.5 GHz band. While the design methodology for the patch antenna element does allow for some selectivity with the received frequency range, it still does pick up unwanted noise. Therefore, a microstrip bandpass filter is combined with the antenna to attenuate the unwanted signals and provide a sufficient gain within the passband. A WEH sub-system implemented into an IoT device could make use of the sub-6 GHz signals that are being transmitted to it as a source of ambient energy. Wireless energy harvesting systems are an emerging technology in the field of communications with applications ranging from wireless sensor networks to battery-less devices. The main objectives of this project are to be able to design, simulate and possibly implement a microstrip filtenna array for the purpose of wireless energy harvesting in an internet of things ecosystem.

Table of Contents

Abstract.....	2
Acknowledgements	4
Chapter 1: Introduction.....	5
1.1: Wireless Energy Harvesting for Internet of Things	5
1.2: Goals and objectives	6
Chapter 2: The Internet of Things	7
2.1: 5G	8
2.2: Energy Harvesting.....	10
Chapter 3: Microwave Integrated Circuit (MIC) Technology.....	11
3.1: The Microstrip Transmission Line.....	11
3.2: Inhomogeneity of the Microstrip.....	12
3.3: Loss	13
3.4: Q Factors.....	13
3.5: The Transmission Line Model.....	14
Chapter 4: Microstrip Patch Antenna Design	15
4.1: Introduction.....	15
4.2: Patch Antenna Element Design Procedure	16
4.3: Results.....	20
4.4: Microstrip Patch Arrays.....	22
4.5: Microstrip Patch Antenna Array 1x2 Design	23
4.6: Microstrip Patch Antenna Array 1x4 Design	24
Chapter 5: The Microstrip Bandpass Filter.....	26
5.1: Filter Technologies	26
5.1.1: Hairpin microstrip bandpass filters	27
5.1.2: Edge-coupled microstrip bandpass filters	27
5.1.3: End-coupled microstrip bandpass filters	28
5.2: Immittance inverters.....	28
5.3.1: Microstrip Bandpass Filter Design Procedure	28
5.3.2: Optimisation.....	33
5.4: Filtenna.....	35
Chapter 6: Resources.....	39
Chapter 7: Project Specification	39
Chapter 8: Ethical and environmental issues.....	40

8.1: 5G panic.....	40
8.2: The ethical and environmental issues of MIC technology	40
Chapter 9: Conclusion	41
9.1: Summary.....	41
Work Plan	43
References	44

Acknowledgements

First and foremost, thanks and praises to God, the Most High, for continuous blessing throughout my research and work to complete the project successfully. I am extremely grateful to [REDACTED] for [REDACTED] unconditional love and support, and for setting such a hard working and motivated example. I wish to thank [REDACTED] for [REDACTED] role in [REDACTED] and preparing me for academic life. I would like to express my appreciation to [REDACTED], my supervisor for his patience, assistance, and support throughout my work. I am fortunate to have such loyal friends around me whom I can confide in such as [REDACTED], who motivate me to keep achieving, with their encouragement and support.

Chapter 1: Introduction

1.1: Wireless Energy Harvesting for Internet of Things

Systems that are able to make use of power that has been collected from energy that would be wasted otherwise, have been implemented in all kinds of technologies from automatic watches to regenerative braking in modern vehicles. With relatively newer technologies such as 5G and the Internet of Things (IoT) being gradually deployed at a large scale, these systems must function within a supporting infrastructure. Therefore naturally, there are concerns about the energy cost of implementing and maintaining such large networks of devices. The power required to maintain these networks would be quite taxing, even when idle. Therefore, wireless energy harvesting (WEH) can be implemented to operate the network in a self-sufficient manner, improving the energy efficiency and prolonging the longevity of the devices.

Internet of Things devices are being designed for 5G to allow for much faster and more reliable data transfer and there are plans to increase 5G coverage in almost every major capital city. These technologies could take advantage of the 5G radio frequencies that will be abundant in the areas with a high concentration of interconnected devices, if they were able to convert that energy into a sustainable stable source of power.

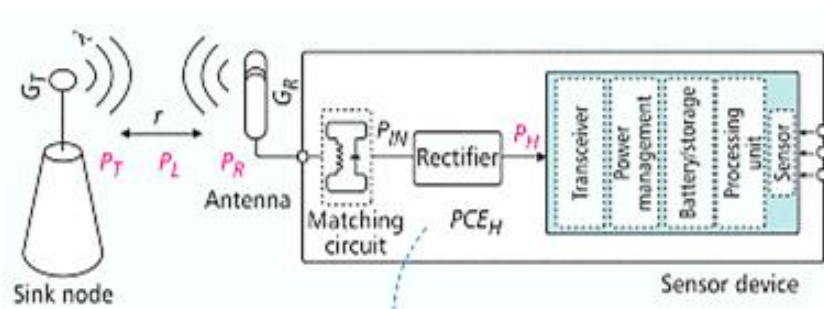


Figure 1: Block Diagram of a wireless energy harvesting sensor device. [6]

The block diagram of a wireless energy harvesting sensor device is shown above in figure 1. The device consists of an antenna, transceiver, WEH unity, power management unit, sensor, processing unit and possibly a battery [6]. In this example, this device would be part of a network of many sensor devices that would all transmit sensory data to the sink node. The WEH sub-system composed of the antenna, matching circuit and rectifier, will receive the transmitted sub-6 GHz 5G signal with the receiving antenna, filter the received signals to isolate the appropriate 3.5 GHz band and then rectify the alternating current (AC) radio frequency (RF) signal into a stable direct current (DC) source. The resulting DC power source can then be used to:

- Supply the communicational and sensory functions of the sensor device.
- Provide a DC bias to amplify components such as amplifiers.
- Store the energy in a battery or some other power storage component.

Commonly mundane devices are slowly becoming 'smart', as the Internet of Things becomes more and more of a reality with every doorbell, lightbulb, and kettle that is released with internet connectivity. With 5G around the corner IoT devices are being designed with 5G connectivity in consideration as it provides greater data speeds and a higher uplink/downlink capacity among other benefits. If you are in an urban environment right now, in a major city, it is likely that there are 5G signals all around you. These radio frequency waves that are being used to transmit data to all kinds of devices can also be converted into useful electrical power. This harvested energy could be used, for example, by charging an internal battery, or even providing a single source of power for a device without any power storage.

The 5G wireless energy harvesting sub-system serves a dedicated purpose independent of the communications and sensory functions of the device described in the example in figure 1. There are three components that would be connected in series to achieve the functions described: the antenna, the filter, and the rectifier. These three components are often combined in different arrangements and often referred to as filtenna or rectenna devices. This project will describe the design and analysis of a filtenna to be deployed in similar applications.

1.2: Goals and objectives

The solution that is explored in this paper is one that seeks to implement wireless energy harvesting sub-systems into IoT networks that are communicating over 5G at frequencies below 6 GHz. A primary objective of this project will be to research 5G Internet of Things wireless energy harvesting sub-subsystems such as the one previously described, as well as learning more about MIC technology, microstrip transmission lines, patch antennas and bandpass filters. The primary objective is to design and simulate a microstrip filtenna at 3.5 GHz. The secondary goals for this project include fabrication, implementation, and experimental verification of the performance of the designed components. However due to the current circumstances and the resources available, some of the secondary goals will not be met. Despite the limitations, this project has resulted in a theoretically approved microstrip filtenna component design that is ready to be manufactured and verified when the appropriate facilities become available.

Listed below are the initial goals for this project, if relevant tools necessary to meet these targets are available.

Primary Goals:

To learn about:

- 5G Internet of things wireless energy harvesting subsystems
- Microstrip patch antennas
- Bandpass filters
- MIC Technology
- Electromagnetic simulation of microstrip lines and their discontinuities.

To design, implement and test:

- Microstrip patch antenna, bandpass filter, filtenna and patch arrays at 3.5 GHz.

Secondary Goals:

- Experimental verification of patch antenna performance characteristics.
- Implement the microstrip patch antenna in 5G IoT wireless energy harvesting system.
- Implement the microstrip patch antenna arrays such as 1x2 and 1x4.
- Evaluation of radiation patterns of designed patch antenna arrays.

Chapter 2: The Internet of Things

Devices that are part of the Internet of Things are increasingly becoming a part of daily life. It is no longer uncommon for generally mundane inanimate objects such as a doorbell, plug socket or a lightbulb to be connected to the internet and conveniently controlled from your smartphone. The Internet of things, commonly abbreviated as IoT, describes a network of interconnected devices that exchange data with other systems over the Internet. The most popular examples of Internet of Things technology are referred to as “smart home” products which include thermostats, light bulbs, and doorbells. Many other previously inanimate household objects have been incorporated into the internet of things as technology improves. The first ever IoT device was a modified soda can vending machine at Carnegie Mellon University in Pittsburgh, Pennsylvania. Developed in the early 1980's, this internet connected appliance introduced the concept interconnected of smart devices.

One of the world's leading cybersecurity software development companies, the developers of Norton Antivirus, published predictions that there could be 11.6 billion IoT devices operational by as soon as 2021, which is expected to almost double by 2025 [7]. The future of many major industries will receive great benefit from Internet of Things, with applications in industries such as:

- Medical and healthcare
- Transportation
- Building Automation
- Manufacturing
- Agriculture
- Maritime
- Environmental Monitoring
- Military

A leading criticism of Internet of Things technology comes from Philp Howard, a professor that cautions people of the threats to cybersecurity, privacy, and potential for social and political manipulation [20]. The main problems of the technology include energy consumption, data storage, environmental, safety and security. With these issues raised concerning power and energy consumption, wireless energy harvesting can be implemented to operate the network in a self-sufficient manner, improving the energy efficiency and prolonging the longevity of the devices.

2.1: 5G

5G is the fifth-generation standard for broadband cellular networks which began in 2019 implemented as a successor to 4G. The sub 6 GHz frequency band that is the chosen band for the designed components, refers to the range of 5G frequencies below 6GHz and above 2.5GHz. The lower bands of 5G use a frequency range like 4G, at around 600–850 MHz and have a coverage like that of 4G. The frequencies ranging from 2.5–3.7 GHz are used for mid-band 5G, which can provide download speeds of around 100–900 Mbit/s and a coverage of several kilometres. High band 5G refers to the frequencies ranging from 25 to 39 GHz, this band can provide download speeds in gigabits per second but with very limited range comparably [16].

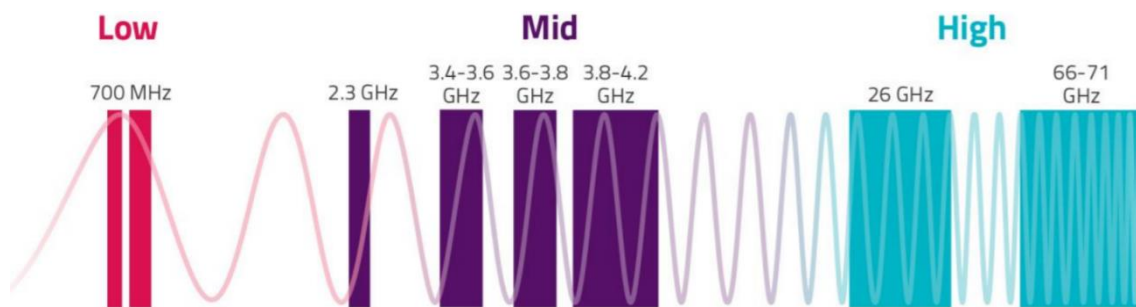


Figure 2: The 5G spectrum pipeline from low to high [25].

The frequency band used in this project is one that is within the mid band, at 3.5 GHz with a bandwidth of 200 MHz, these frequencies between 3.4 GHz and 3.6 GHz are available in many urban centres including central London. In December of 2017 the leading telecommunications company Vodafone, conducted a 5G test at the 3.5 GHz range using the latest 5G antenna technology, in a joint venture with Ericsson and King's College London [25].

Commercially, the most deployed 5G frequency band is the 3.5 GHz frequency band. 5G networks that are operating at around the 3.5 GHz can be deployed at a faster rate than other bands because existing infrastructure from the previous generation can be easily expanded as many 4G networks also made use of MIMO systems [23]. The coverage of this 3.5 GHz band is limited by the propagation properties of higher frequency radio waves. However, there are many techniques that are implemented to mitigate the effects of these issues such as beam forming, beam tracking and massive MIMO. Earlier networks deployed at the 3.5 GHz range have used smaller frequency ranges, with the most popular channel width being the maximum 100 MHz [24].

The use of multiple antenna elements arranged in an array as part of the filtenna would work in conjunction with multiple-input and multiple-output (MIMO) and massive MIMO technology. MIMO networks use two to four antennas in an array, whereas massive MIMO can use much more antennas like an arrangement of 64x64. The filtenna component will be designed and analysed with different antenna array configurations up to 1x4, which is suited for existing sub-6 GHz 5G MIMO systems that already deployed and transmitting these signals in places like London.

When analysing MIMO systems, the most important things to consider include determining the received signal power, capacity of the downlink/uplink and accurately modelling the propagation path loss. The procedure to calculate these characteristics of a MIMO network is carried out using the following equations.

$$S = P_t + G_t + G_r - L_s \quad (1)$$

The received signal power (S) in decibels is calculated with the formula shown above in equation (1). Where the transmitted power (P_t) summed with the transmitting and receiving antenna gains (G_t and G_r), and then finally the free space loss (L_s) is subtracted.

$$L_s = 32.45 + 20 \log f_{\text{MHz}} + 20 \log d_{\text{km}} \quad (2)$$

The free space path loss model shown above in equation (2) is one of the two methods for modelling propagation loss developed by Samsung. Where the free space path loss is calculated in decibels.

$$C_{\text{downlink}} = M_{\text{TX}} B \log_2 \left[1 + \left(\frac{S}{N} \times \frac{K_{\text{RX}}}{M_{\text{TX}}} \right) \right] \quad (3)$$

$$C_{\text{uplink}} = N_{\text{TX}} B \log_2 \left[1 + \left(\frac{S}{N} \times \frac{L_{\text{TX}}}{N_{\text{RX}}} \right) \right] \quad (4)$$

The formulas (3) and (4) are used to calculate the downlink and uplink capacity in bits per second, of the connection established between the receiver and transmitting antennas in the MIMO network. Where the number of receiving/transmitting antennas are (M_{TX} , N_{TX} , K_{RX} and L_{TX}), the bandwidth is (B) and the signal to noise ratio is ($\frac{S}{N}$).

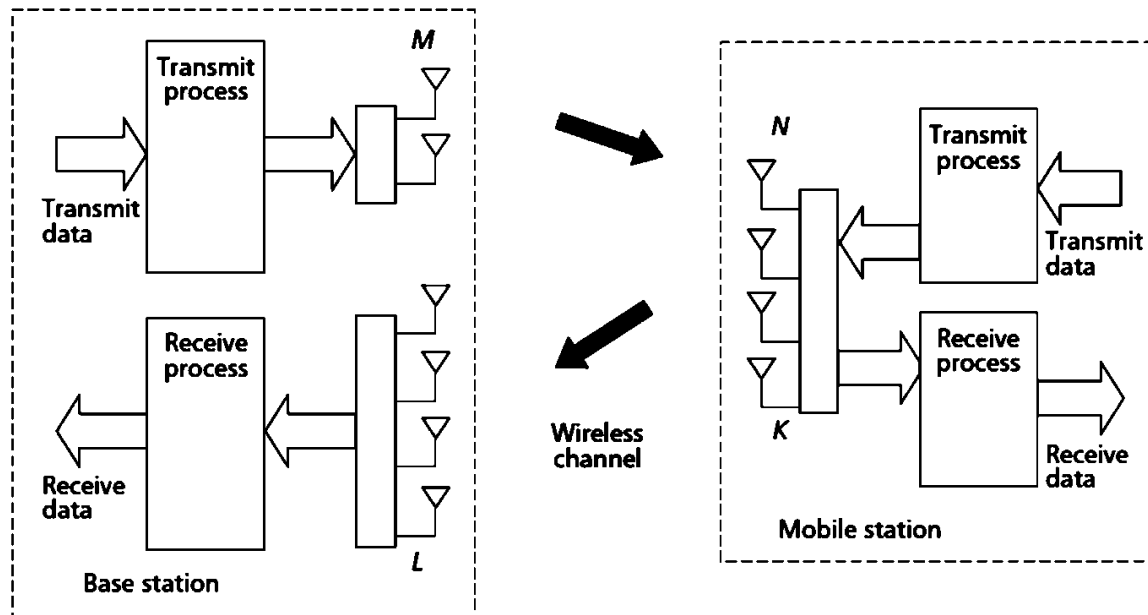


Figure 3: A typical MIMO network connection from base station to mobile. [26]

2.2: Energy Harvesting

Energy harvesting is commonly defined as the conversion of ambient energy into electrical energy. Ambient energy is the energy that is all around us, existing in many forms such as thermal, chemical, electrical, mechanical, etc [8]. Wireless energy harvesting (WEH) is known as the conversion of ambient electro-magnetic RF energy into useful electrical energy for devices [8]. The popularisation of wireless power transmission can be attributed to the inventor Nikola Tesla, with his experiments transmitting power using large transformers now known as Tesla coils. From 1890's onwards, Nikola Tesla would go on to experiment with all kinds of ideas ranging from a wireless lighting system to finally introducing his "World Wireless System", which promised to provide an AC power supply with very little loss that can be accessed from anywhere in the world with a similar tower construction [17]. Tesla's achievements built upon the work of early 1800's pioneers such as André-Marie Ampère, Michael Faraday and James Clerk Maxwell to name a few.

The WEH unit that is to be designed and simulated is one that will be able to generate useful power from received 5G signals at a frequency of around 3.5 GHz. The received power can be increased by increased the gain of the receiving antenna which is done by increasing the number of antenna elements in the array, this is important when considering the benefits of implementing a WEH subsystem because the amount of power that the device is able to receive can be increased within limitations, due to the physical size of the antenna array being too large to fabricate with the regular tools.

Chapter 3: Microwave Integrated Circuit (MIC) Technology

3.1: The Microstrip Transmission Line

Initially developed as a successor to the stripline, microstrip technology was developed by D. Grieg and H. Engelmann. The two engineers and senior members at the Institute of Radio Engineers introduced the microstrip as “A New Transmission Technique for the Kilomegacycle Range” with their paper published in the periodical “Proceedings of the IRE” in 1952 [14]. The main applications of the microstrip transmission line can be classified under radar and wireless communication systems. This transmission line can be manufactured with a process very similar to that of the method for fabricating printed circuit boards, commonly abbreviated as PCBs. Circuits that are designed to operate at microwave frequencies are known as microwave integrated circuits or MIC circuits.

The microstrip transmission line is designed with a dielectrically inhomogeneous structure, composed of a conductor fixed upon a dielectric substrate layer that is mounted onto a conductive base plate, which acts as the ground plane. At least two microstrip lines lying parallel, in close proximity to one another are referred to as coupled. In planar designs for microstrip lines, the conductor width can be changed to adjust the impedance. The wide range of impedances that are achievable when designing a microstrip transmission line make them an appropriate component for use in the design of filters.

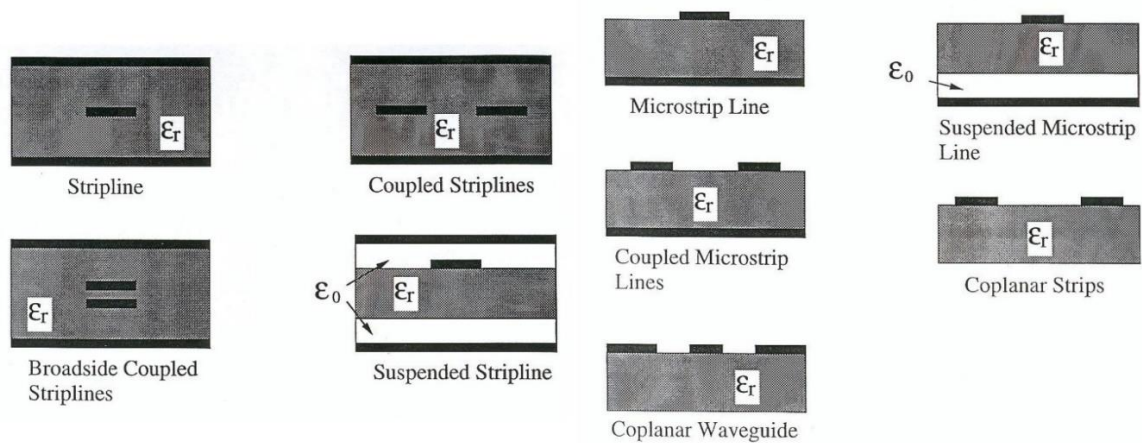


Figure 4: Cross section of different MIC technologies.[1]

Among the parameters that must be considered when describing its behaviour are the effective dielectric constant (ϵ_{eff}), the characteristic impedance (Z_0) and the guided wavelength (λ_g). Listed below are the expressions used to derive the relevant parameters. The characteristic impedance and effective dielectric constant be obtained using one of two formulas depending on the line width to substrate height ratio $\frac{W}{h}$.

If $\frac{W}{h} < 1$:

$$Z_0 = \frac{60}{\sqrt{\epsilon_{eff}}} \ln \left(8 \frac{h}{W} + 0.25 \frac{W}{h} \right) \quad (5)$$

$$\epsilon_{eff} = \frac{\epsilon_r + 1}{2} + \frac{\epsilon_r - 1}{2} \left[\left(1 + \frac{12h}{W} \right)^{-\frac{1}{2}} + 0.049 \left(1 - \frac{W}{h} \right)^2 \right] \quad (6)$$

If $\frac{W}{h} > 1$:

$$Z_0 = \frac{\frac{120\pi}{\sqrt{\epsilon_{eff}}}}{\frac{W}{h} + 1.393 + 0.667 \ln \left(\frac{W}{h} + 1.444 \right)} \quad (7)$$

$$\epsilon_{eff} = \frac{\epsilon_r + 1}{2} + \frac{\epsilon_r - 1}{2} \left(1 + 12 \frac{h}{W} \right)^{-\frac{1}{2}} \quad (8)$$

The guided wavelength can be described by the following expression, where λ_0 is the wavelength of the resonant frequency of the microstrip line.

$$\lambda_g = \frac{\lambda_0}{\sqrt{\epsilon_{eff}}} \quad (9)$$

3.2: Inhomogeneity of the Microstrip

The inhomogeneity of the microstrip transmission line is a result of the electromagnetic waves passing through the line, also propagating through two mediums of different dielectric constants. The dielectric substrate layer will naturally have a greater dielectric constant than that of air surrounding it, resulting in the propagation velocity being somewhere between the speed of electromagnetic waves in air and the speed of the waves in the substrate. The effective dielectric constant (ϵ_{eff}), of the microstrip is used to describe this behaviour, with its value representing the dielectric constant of an equivalent homogeneous medium that would provide the same propagation velocity.

Another consequence of this inhomogeneous behaviour is that the dominant mode for microstrip is known as quasi-TEM. At frequencies other than zero, the microstrip transmission line will not support a true transverse electromagnetic (TEM) wave, this is because both E and H fields will have components perpendicular to the direction of radiation.

As the frequency increases, the effective dielectric constant of the microstrip gradually reaches that of the substrate within, causing the rate at which the waves propagate through the line to decrease. This leads to a phenomenon in which the phase velocity of the electromagnetic waves propagating through the transmission line are directly related to the frequency of the wave. Therefore, the microstrip is said to be dispersive, regardless of the dispersive properties of the chosen substrate. [18]

This inhomogeneous structure of the microstrip transmission line has other consequences for its behaviour, including:

- The characteristic impedance of the line varies slightly as the frequency changes.
- The wave impedance is different in different places in the line.
- Radiation occurs at the discontinuities such as steps in width, bends, and junctions.

3.3: Loss

Power loss in the transmission line occurs in different forms such as conductor loss, dielectric loss, radiation loss and surface wave propagation. Conductor and dielectric losses are dissipative effects, whereas the radiation loss and surface wave propagation are parasitic effects that only occur at the discontinuities such as bends or steps in width. The main losses that will be measured throughout the design process will be the reflection loss ($S(1,1)$) and the transmission loss ($S(2,1)$). The transmission loss is simply the decrease in intensity due to the propagation and reflection loss occurs when the RF currents are being partially reflected back to the source, which mostly happens at discontinuities or impedance mismatches in the transmission line.

The dissipative losses are summed together to determine the constant of attenuation (α). The Q-factor can also be determined in terms of the attenuation constant.

3.4: Q Factors

There are usually three quality factors that can be defined; unloaded, loaded and external. High-Q oscillators tend to be more stable. The suspended microstrip configuration, which can be seen in figure 4, has a layer of air separating the substrate and the ground plane. This adjustment to the standard configuration provides a higher Q factor than the microstrip line.

Transmission Line Structure	Characteristic Impedance Range (Ω)	Unloaded Q Factor (Q_u) at 30 GHz	Frequency Range (GHz)
Microstrip	20 - 125	250	Up to 110
Coplanar Waveguide	25 - 150	100	Up to 100
Suspended Stripline	40 -150	Up to 600	Up to 110
Suspended Microstrip	40 -150	500 -1500	Up to 110
Finline	10 -400	500	Up to 110
Image Line	≈ 26	2700	Up to 110

Table 1: Properties of various transmission line structures.

Comparing the various types of transmission lines against each other, different transmission line structures behave differently within a given frequency range. The differences in characteristic impedance and unloaded Q-factor can be compared against each other as shown in the table above. These properties inherent to the different transmission lines structures may become important considerations if the results of the chosen microstrip filtenna designs is lacking something in Q-factor or characteristic impedance range.

3.5: The Transmission Line Model

The transmission line model is the simplest to execute of the alternatives. It provides a useful insight into the behaviour of the antenna, but it is not as accurate. The microstrip patch antenna is modelled as an impedance separated by two discontinuities. The transmission line model considers the fringing effects, resonant input resistance and conductance among other key properties. Along the edges of the microstrip patch, the electromagnetic fields will exhibit fringing, the amount of fringing that occurs is dependent on the physical dimensions of the patch, W and L , and the height of the substrate t . Fringing must be considered when modelling the microstrip antenna because this effect has an influence on the resonant frequency [15]. Due to this fringing effect at the edges of the antenna, the length of the patch can be extended by Δl on each side. These lengths are summed together to produce an effective length for the microstrip patch. The value of Δl is a function of the effective dielectric constant and the patch width to substrate height ratio. The effective dielectric constant of the antenna increases with the frequency of operation. As the frequency increases, the microstrip patch antenna behaves more like a dielectrically uniform and homogenous material, and the effective dielectric constant slowly approaches the dielectric substrate constant.

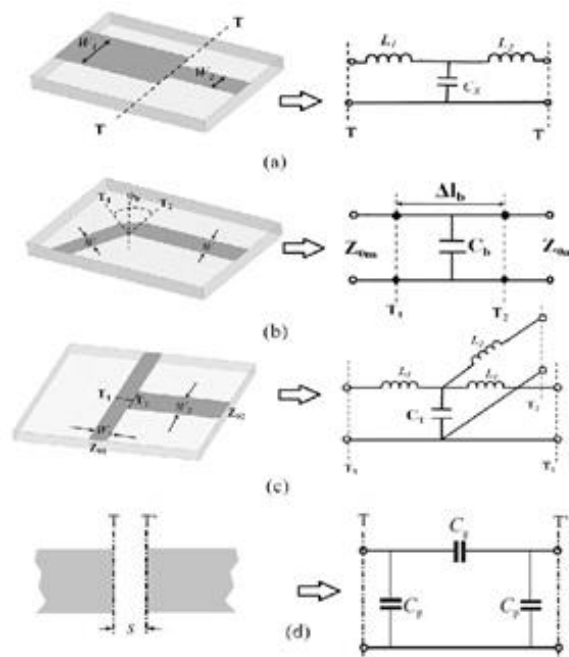


Figure 5: Different types of microstrip line discontinuities and their equivalent circuits. [19]

Shown above in figure 5 are some equivalent circuits that are derived from the transmission line model to describe certain sections of microstrip. The design procedure that is to be followed when using the transmission line model for a microstrip patch antenna is described in the design methodology section.

Chapter 4: Microstrip Patch Antenna Design

4.1: Introduction

Composed from a metallic patch fixed upon a layer of dielectric substrate mounted onto a metallic ground plane [1]. The role of antennas in general is to act as an interface between radio waves and radio frequency currents that are induced in the metal. Since its introduction to the field the rectangular patch antenna has become increasingly widespread in the wireless communications industry. They are the most used type of microwave antenna due to their relatively compact structure and efficiency. These antennas can be either circular or rectangular in shape and easily made at low costs. They are often fixed to the exterior of vehicles as well as inside mobile phones due to their ability to be shaped to surfaces and their low profile. These benefits greatly outweigh the negatives for most commercial applications, which is partly why the microstrip patch antenna has become so popular.

The disadvantages of the microstrip patch antenna include its comparatively low received power, efficiency and narrower bandwidths. Energy is lost through wasteful radiation that occurs at the feeds, junctions, and surface waves along the materials. High-quality substrates are difficult to source and there is an issue with the difficulty of obtaining a high polarization purity. Microstrip patch antennas can also be quite large physically, at very high frequency bands, arrays with many antenna elements also require complex feeding systems that occupy a large portion of the overall physical dimensions. Be that as it may, the strengths of the microstrip patch antenna greatly outweigh its weaknesses, which is demonstrated by how popular they are as an RF antenna solution. The advantages of the microstrip patch antenna include their thin profile, light weight, easy and expensive to manufacture design. The patch antenna is conformable to non-planar surfaces, durable and can tolerate high temperatures. Being compatible with MMIC designs, their high adaptability to different impedances, frequencies, and polarizations makes the microstrip patch antenna an ideal candidate for a filtenna device.

Microstrip patch antennas come with a variety of different input lines including the microstrip line feed, the aperture-coupled feed and the proximity coupled feed. These input lines, referred to as feeds, act as an interface to connect to another component and transfer the RF currents induced in the antenna. The main parameters describing the microstrip patch antenna include the input impedance, resonant frequency, radiation resistance, bandwidth, and radiation pattern.

There are two methods that can be used for analysis and design of a microstrip patch antenna, the transmission line model and the cavity model. These methods

are used to produce a mathematical model of the antenna and enable simulation of its operation. The transmission line model treats the patch antenna as a very wide transmission line terminated by the radiation impedance. This method can only predict the properties of the antenna approximately because the formulas themselves are approximations and designed to reproduce measured data. The cavity model is used for microstrip patch antennas with feeds going through the substrate and ground plane, typically terminating in a coaxial connector.

4.2: Patch Antenna Element Design Procedure

The method used to determine the physical dimensions of the microstrip patch antenna can only predict these properties approximately, this is because the formulas derived from the transmission model are approximations or are created to fit to existing measurements. Using the appropriate formulas, an initial value for the physical dimensions of microstrip patch antenna will be calculated and then the design will be transferred to ADS where the model can be simulated, tuned, and tested. A physical width of the patch antenna element can be determined making use of the formula (10). The antenna is designed to operate at a resonant frequency (f_r) of 3.5 GHz. The dielectric constant ϵ_r , is a result of the dielectric properties of the chosen substrate material. Composite micro-fibre glass has been measured to have a dielectric constant of 2.2. An initial value for the physical width of the patch antenna element can be calculated with following formula, where c is the speed of light ($c = 3 \times 10^8$).

$$W = \frac{c}{2f_r} \left(\frac{\epsilon_r + 1}{2} \right)^{-\frac{1}{2}} = \frac{3 \times 10^8}{2 \times 3.5 \times 10^9} \left(\frac{2.2 + 1}{2} \right)^{-\frac{1}{2}} = 33.882 \text{ mm} \quad (10)$$

The effective dielectric constant can be determined with the following calculation using the substrate constant and the height of the substrate along with the width calculated in the previous calculation. The height of the substrate is to be 0.510mm. Depending on the value of $\frac{W}{h}$, the width of the antenna element divided by the height of the substrate, the appropriate formulas are used to calculate the characteristic impedance and the effective dielectric constant of the patch antenna.

$$\epsilon_{eff} = \frac{2.2 + 1}{2} + \frac{2.2 - 1}{2} \left(1 + \frac{12 \times 0.51 \times 10^{-3}}{33.88 \times 10^{-3}} \right)^{-\frac{1}{2}} = 2.152 \quad (11)$$

$$\begin{aligned} Z_0 &= \frac{60}{\sqrt{\epsilon_{eff}}} \ln \left(8 \frac{h}{W} + 0.25 \frac{W}{h} \right) \\ &= \frac{60}{\sqrt{2.152}} \ln \left(8 \frac{0.51 \times 10^{-3}}{33.88 \times 10^{-3}} + 0.25 \frac{33.88 \times 10^{-3}}{0.51 \times 10^{-3}} \right) = 115.221 \Omega \end{aligned} \quad (12)$$

A value for the physical length of the patch is calculated using the following formulas. The fringing length extension length Δl and the physical length L can be combined to obtain an effective length L_e .

$$\Delta l = 0.412h \left(\frac{\epsilon_{eff} + 0.3}{\epsilon_{eff} - 0.258} \right) \left(\frac{\frac{W}{h} + 0.264}{\frac{W}{h} + 0.8} \right)$$

$$= 0.412h \left(\frac{2.152 + 0.3}{2.152 - 0.258} \right) \left(\frac{\frac{33.88 \times 10^{-3}}{0.51 \times 10^{-3}} + 0.264}{\frac{33.88 \times 10^{-3}}{0.51 \times 10^{-3}} + 0.8} \right) = 269.849 \mu mm \quad (13)$$

$$L = \frac{c}{2f_0 \sqrt{\epsilon_{eff}}} - 2\Delta l = \frac{3 \times 10^8}{2 \times 3.5 \times 10^{-9} \times \sqrt{2.152}} - (2 \times 270 \times 10^{-6}) = 28.674 mm \quad (14)$$

$$L_e = L + 2\Delta l = 28.674 \times 10^{-3} + 2 \times 28.674 \times 10^{-3} \quad (15)$$

The input impedance R_{in} , can be determined by making use of an equivalent circuit to model the input transmission line. Depending on the condition $W < \lambda_0$ there are two formulas that can be used to obtain the impedance at the input R_{in} . In this case the width of the patch antenna element is less than the wavelength λ_0 .

Where $\lambda_0 = c/f_r = \frac{3 \times 10^8}{3.5 \times 10^9} = 85.71 mm$ and therefore the condition of $W < \lambda_0$ is met, the following formulas are used.

$$R_{in} = \frac{45\lambda_0^2}{W^2} = \frac{45 \times (85.71 \times 10^{-3})^2}{(33.88 \times 10^{-3})^2} = 288 \Omega \quad (16)$$

$$Z_T = \sqrt{R_{in} \times Z_{in}} = \sqrt{288 \times 50} = 120 \Omega \quad (17)$$

$$\lambda_g = \frac{\lambda_0}{\sqrt{\epsilon_{eff}}} = \frac{85.71 \times 10^{-3}}{\sqrt{2.152}} = 58.427 mm \quad (18)$$

With these initial calculations, the remaining values needed to simulate the antenna are the width and length of both the input and quarter wavelength transformer transmission lines. These values can be determined using the software tool integrated into ADS known as LINECALC.

LineCalc/D:\Media\Documents\FinalProject\linecalcproj.lcs

File Simulation Options Help

Component
Type: MLIN ID: MLIN: MLIN_DEFAULT

Substrate Parameters
ID: MSUB_DEFAULT

Er	2.200	N/A
Mur	1.000	N/A
H	0.510	mm
Hu	3.9e+34	mil
T	0.018	mm
Cond	4.1e7	N/A
TanD	0.001	N/A
Rough	0.000	mil
DielectricLossModel	1.000	N/A
FreqForEpsrTanD	1.0e9	N/A
LowFreqForTanD	1.0e3	N/A
HighFreqForTanD	1.0e12	N/A

Physical
W: 1.546240 mm
L: 14.321800 mm

Synthesize Analyze

Electrical
Z0: 50.000 Ohm
E_Eff: 82.408000 deg

Calculated Results
K_Eff = 1.874
A_DB = 0.018
SkinDepth = 0.001

Component Parameters
Freq: 3.500 GHz
Wall1: mil
Wall2: mil

Values are consistent

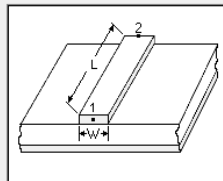


Figure 6: LineCalc UI, synthesising the input line.

Using LINECALC, the appropriate values describing the electrical and substrate properties of each microstrip line are entered into the user interface as shown above in figure 6. The physical dimensions are obtained by running the “Synthesize” function. The synthesis procedure provides the width W , for a corresponding value of the characteristic impedance Z_0 , for each transmission line. The input impedance as taken from the project specification is to be 50Ω and the impedance for the quarter wavelength transformer is 120Ω . A new schematic is created in ADS, passing the appropriate values to each component accordingly and providing the appropriate simulation and substrate parameters. With a complete circuit schematic, the behaviour of the antenna can be simulated and compared to the specification.

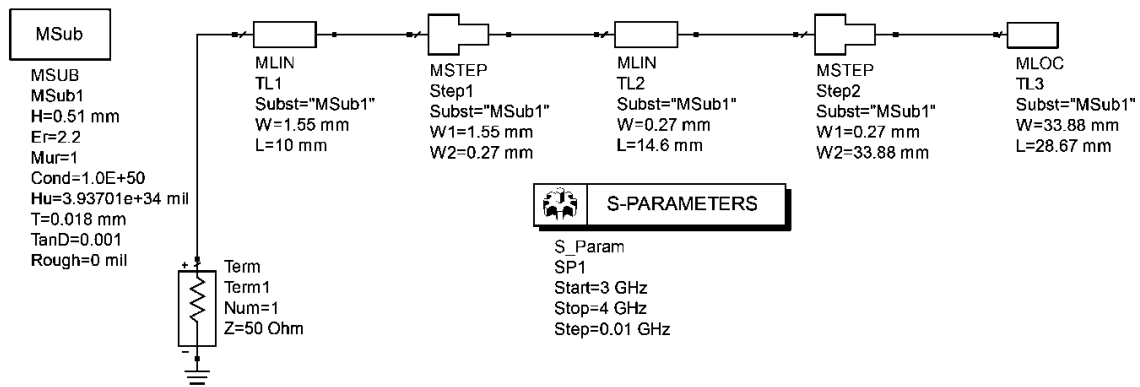


Figure 7: Schematic circuit diagram of a microstrip patch antenna element.

The resultant microstrip line schematic diagram depicted above in figure 7 is created in ADS using values shown in the previous calculations and some obtained using another software tool known as LINECALC. The circuit is terminated by a Microstrip Open-Circuited Stub, referred to as MLOC, on one end. A port termination with an impedance of 50 Ohms and its negative terminal connected to ground is on the other. The MLOC component represents the rectangular patch, inheriting its physical dimensions (W and L), which were determined in the previous calculations. The components Step1 and Step2 represent a change in width of the microstrip lines, with the documentation describing the component MSTEP to be an abbreviation for Microstrip Step in Width. The microstrip line (MLIN) components TL2 and TL1 represent the quarter wavelength transformer and input transmission lines respectively, with their widths having been determined with LINECALC. The length of the quarter wavelength transformer is a quarter of the wavelength λ_g and any changes in length to the input line TL1 has little effect on the overall behaviour.

The components in the schematic diagram excluding the port termination to ground, contain the substrate parameter MSub1. This microstrip substrate component is required for all microstrip components and contains the properties of the substrate required to simulate its behaviour. The S-Parameters component contains the parameters that are to be defined for simulation. An appropriate range of 1 GHz is chosen with the resonant frequency in the centre, and a step of 0.01 GHz is chosen to provide a sufficient resolution for the plotted results.

4.3: Results

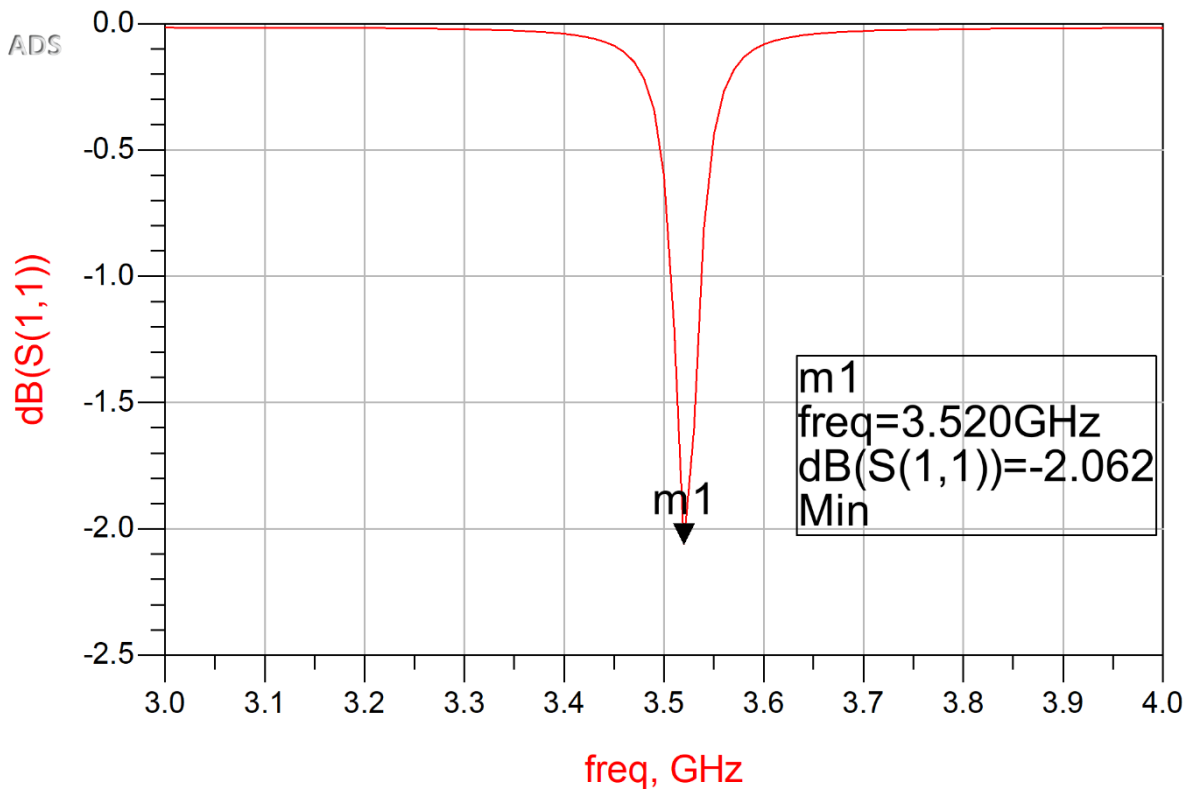


Figure 8: Reflection Loss over a range of frequencies in a microstrip patch antenna.

Simulating the circuit schematic within the defined parameters provides the graph shown in figure 8, which shows the reflection loss in decibels over a range frequency from 3 to 4 GHz. The lowest point on the graph appears to be at 3.52 GHz, which is 20 MHz off the desired resonant frequency defined in the specifications for the antenna. At the designed patch antenna's resonant frequency, a reflection loss of -2.062 dB is observed in the results of the simulation. This means that at the resonant frequency, the microstrip patch antenna can be expected to reflect away 62% of the energy it receives. The conversion from decibels to percentage loss is calculated with the following, where d is the value of reflection loss in decibels and p is the percentage loss. $p = 10^{\frac{d}{10}} \times 100$ (19)

A layout can be generated from the schematic which provides a more visually appealing diagram that shows the overall shape of the antenna. With a total length of 53.28 mm and width of 33.88 mm.

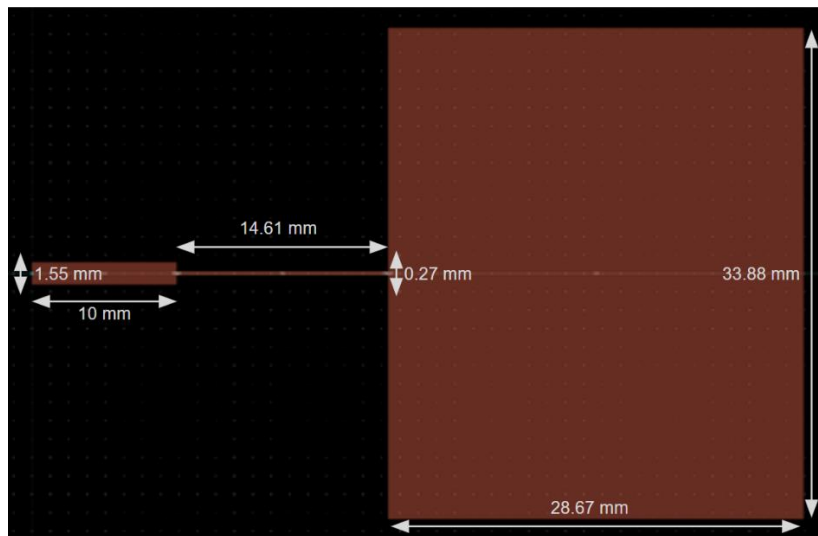


Figure 9: Rectangular patch layout

Further work could be done to tune the behaviour of the design, further decreasing the transmission loss. Fabrication of the patch antenna would make use of a ProtoMat C60 to plot the design onto a printed circuit (PCB). A Vector Network Analyzer would then be used to analyse and measure the behaviour the designed patch antenna, however antenna component not be worked on any further due to the ongoing COVID-19 situation. Which has caused a reduced availability in crucial software licenses and equipment used generate a layout and further simulate and analyse the characteristics.



Figure 10: ProtoMat C60 Circuit Board Plotter (right) and Vector Network Analyzer (left).

4.4: Microstrip Patch Arrays

Microstrip patch arrays come in a range of elaborate designs, with multiple identical antenna elements and each patch requiring a connection. The resulting power distribution/beam forming networks come in two varieties, the series fed and the parallel fed microstrip patch arrays.

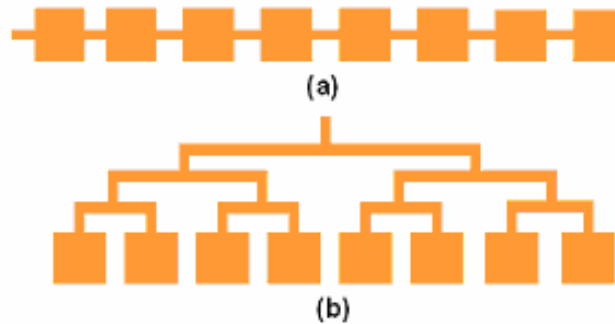


Figure 11: Example of a series fed (a) and parallel fed (b) microstrip patch antenna array.[21]

The parallel fed microstrip patch array network makes use of Wilkinson Power Dividers to split the input signal into two output signals with equal phase or combine two signals of equal phase into one. This power dividing component relies on quarter wavelength transformers to match the ports. A single resistor is used across the two ports to match the phases and fully isolate the ports from each other at the centre frequency, if power were to be connected to port 2, ideally it would all be dissipated in heat across the capacitor.

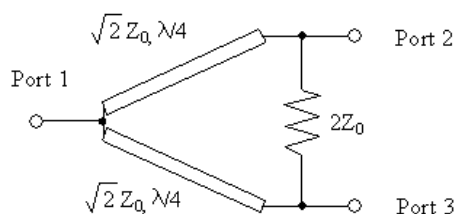


Figure 9: An ideal two-port Wilkinson power divider.[22]

When a signal enters port 1, it splits into two signals of equal amplitude and phase. With each terminal of the resistor between ports 2 and 3 at the same voltage, no current flows through it and the resistor therefore decoupled from the input. The output ports will add in parallel at the input, so they must be transformed to double that of the characteristic impedance. The quarter-wave transformers in each leg accomplish this; without the quarter-wave transformers, the combined impedance of the two outputs at port 1 would be $Z_0/2$. The characteristic impedance of the quarter-wave lines must be equal to $1.414 \times Z_0$ so that the input is matched when ports 2 and 3 are terminated in Z_0 . When connected in series to the bandpass filter, the Wilkinson power dividers in the antenna array will be acting to combine the power received from each antenna. In this case, it splits the power equally between the port and the resistor. The resistor is decoupling the ports 2 and 3, for a

signal input at either port 2 or 3, half the power is dissipated in the resistor and half is delivered to port 1. [22]

4.5: Microstrip Patch Antenna Array 1x2 Design

The single microstrip patch antenna element can be duplicated and connected with multiple other identical antenna elements to increase the received gain. To connect many antenna elements to operate together, an impedance matching RF circuit based on the Wilkinson power divider is implemented. The circuit diagram for a 1x2 microstrip patch antenna array is designed by placing two antenna elements and connecting them with a 50Ω resistor across the input lines. This resistor along with the rest of the components connecting these elements to a common input, are part of a supporting matching circuit that is implemented to reliably match and isolate the two incoming RF signals received by the antennas.

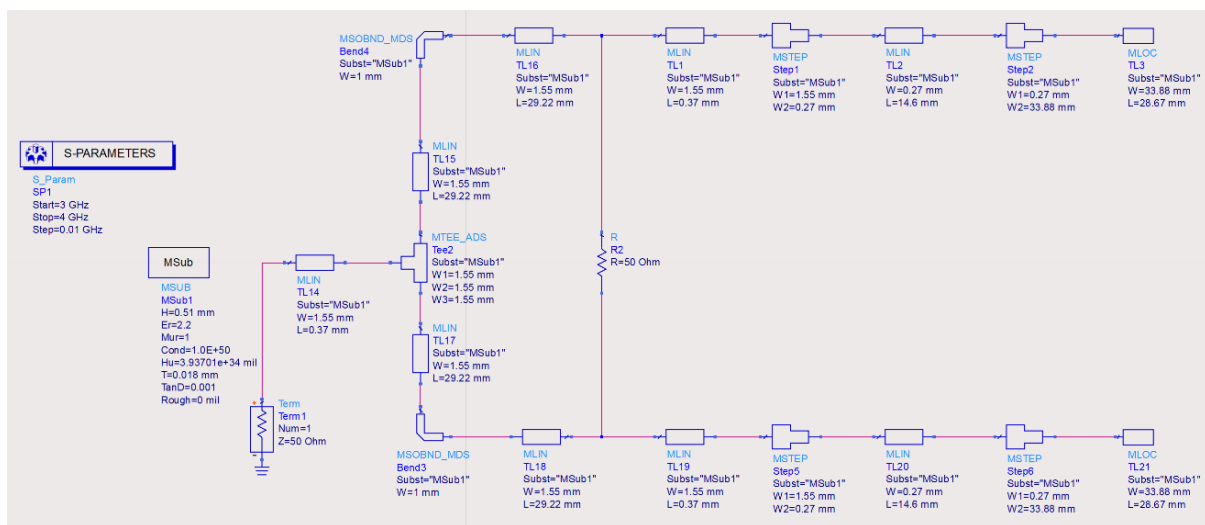


Figure 12: Schematic circuit diagram of a 1x2 microstrip patch antenna array.

The microstrip line components TL15, TL16, TL17 and TL18 are all assigned the same properties. The widths remain 1.55 mm to keep the characteristic impedance of the lines matching with the input impedance for the antenna elements. The design of the antenna array makes use of a Wilkinson power Divider circuit to split the input signal into two output signals of equal phase, the resistor across the two ports allows for them to be matched and isolated at the centre frequency. The resulting graph from performing the simulation shows an improved loss compared to the previous single element design. The lowest point is approximately -1.32 dB at 3.51 GHz.

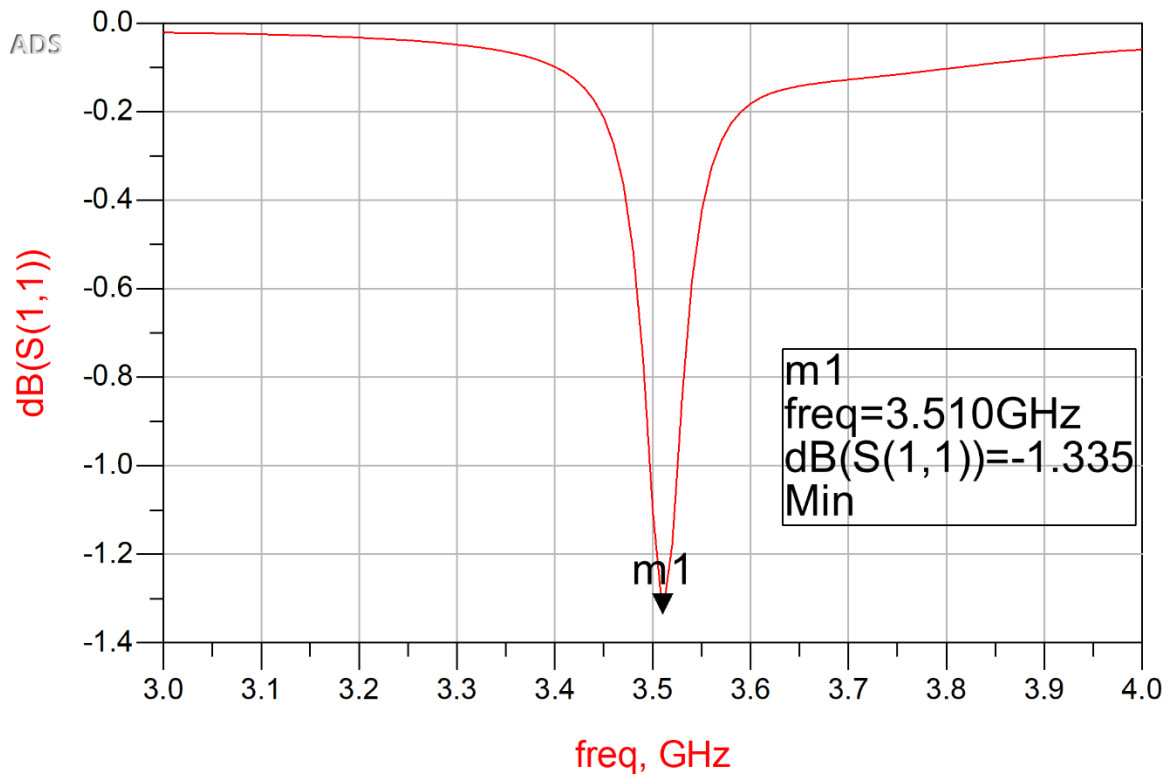


Figure 13: Reflection Loss over frequency of a 1x2 patch antenna array.

Comparing the results of the simulation of the 1x2 antenna array to that of the single antenna elements, the resonant frequency is more accurate to the specification, but the minimum reflection loss is much greater. At the resonant frequency for the 1x2 antenna array, the minimum reflection loss is greater, at -1.335 dB almost 74% of the energy received is lost due to reflection. This is not a desirable amount of loss therefore the design of the initial single antenna element, which is duplicated to create the arrays, can be tuned and adjusted to decrease the loss due to reflection.

4.6: Microstrip Patch Antenna Array 1x4 Design

The received power gain has a direct relationship with the number of elements in the antenna array. Doubling the number of antenna elements again, designing an array made of 4 antennas combined with matching circuits should further improve losses and power gain. A similar process is repeated to before however an identical matching circuit it used to combine the two previously designed 1x2 arrays into one common transmission line in a fractal manner.

The plot shows the return loss $\text{dB}(S(1,1))$ as a function of frequency in GHz. A sharp resonance dip is observed at 3.500 GHz, reaching a minimum value of -1.999 dB. The plot includes a grid and a data box for the minimum point.

Point	freq, GHz	$\text{dB}(S(1,1))$
m1	3.500	-1.999

Figure 15: Reflection Loss over frequency for a 1x4 antenna array.

Simulating the circuit schematic within the defined parameters provides the graph shown in figure 15, which shows the reflection loss in decibels over a range of frequencies from 3 to 4 GHz. The lowest point on the graph appears to be a reflection loss of about -2dB at 3.5 GHz which is accurate to specified resonant frequency and the increased number of antenna elements is sure to have increased the received power gain. A reflection loss of -1.999 dB at the resonant frequency of 3.5 GHz means a 63% loss in energy due to reflection in the 1x4 antenna array.

Chapter 5: The Microstrip Bandpass Filter

5.1: Filter Technologies

The role of filters in general is to allow the desired frequencies to pass while attenuating others. Arrangements of microstrip filters come in various shapes and sizes with the decision to use the lumped element bandpass filter mostly influenced by the simplicity of its fabrication. The lumped element parallel coupled filter is made up of many coupled microstrip lines that act as resonators. The chosen frequencies that can pass through the filter un-attenuated depend on the design of the filter and its intended application. The main types of filters are the lowpass, high pass, bandpass and bandstop filters.

Filters exist in various configurations and make use of different technologies to achieve the same solution. There are two major classifications for typical filters, non-planar and planar. Non-planar filters include the coaxial, waveguide and dielectric filters. Planar or printed filters include the microstrip, stripline, suspended stripline, and others. Microstrip filters have been deployed in mobile cellular radio, satellite communications and radar systems applications which just about covers all modern-day wireless communications. Advanced communication systems require filters that are compact and capable of handling high power, have low loss and high Q factor.

The chosen design is a microstrip lumped element parallel-coupled bandpass filter. The chosen arrangement of microstrip resonators uses the available frequency resources effectively and allows for high quality communication at narrow bandwidths [3].

Filters that are used for 5G must be able to:

- Implement complex multiplexing
- Maximize the efficiency of the power amplifier efficiency and receiver sensitivity
- Perform reliably for a long period of use.
- Be available for prototyping and product development. (Time-to-Market)
- Easily implemented into existing solutions, adapted to be used with different wireless communication standards(Ease of integration)

Theoretically they are described and modelled in terms of equivalent circuits. Microstrip bandpass filters come in all kinds of arrangements including the end coupled, edge coupled, hairpin, interdigital and combline configurations.

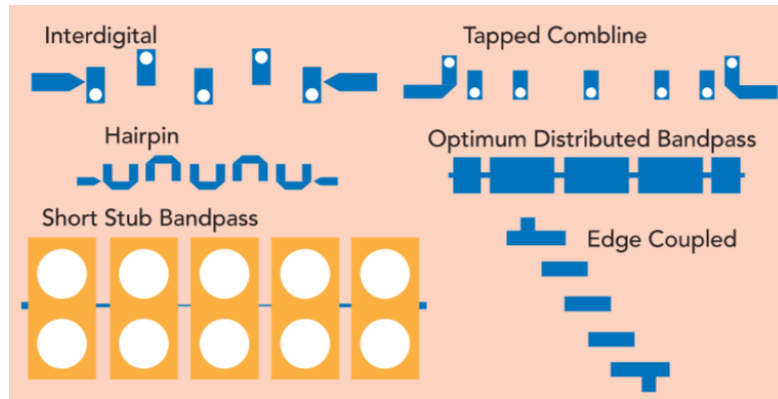


Figure 16: Different types of 5G microstrip filters.[1]

5.1.1: Hairpin microstrip bandpass filters



Figure 17: Generalised hairpin microstrip bandpass filter structure.[27]

The hairpin configuration can support frequency ranges of below 10 GHz and bandwidths ranging from 4% to 30% of the resonant frequency. The hairpin microstrip bandpass filter is able to provide a wide bandwidth and a flat passband slope however this arrangement does have a longer overall width in comparison to other structures.[27]

5.1.2: Edge-coupled microstrip bandpass filters



Figure 18: Generalised edge-coupled microstrip bandpass filter structure.[27]

The edge-coupled microstrip bandpass filter can support frequency ranges below 10 GHz and bandwidths ranging from 4% to 20% of its resonant frequency. The main advantage of the edge-coupled filter structure is that it is able to reduce the overall length of the filter by almost half in comparison to an end-coupled filter, as well as providing a wider bandwidth. The Edge-coupled configuration also provides a symmetrical frequency-response curve; however, the passband slope is much higher in contrast to other microstrip bandpass filter structures.[27]

5.1.3: End-coupled microstrip bandpass filters



Figure 16: Generalised end-coupled microstrip bandpass filter structure.[27]

End-coupled microstrip bandpass filters can also support frequency ranges below 10 GHz however the typical bandwidths supported are between 2% and 10% that of the resonant frequency. This is much shorter possible bandwidth in comparison to the other microstrip bandpass filter structures, however this does make the end-coupled configuration ideal for narrowband applications. This choice of structure does increase the overall filter length, but the width of the filter can be much thinner due the widths of the resonators all being the same. Generally, a higher insertion loss is observed in comparison to other structures however the end-coupled configuration does provide a higher rejection roll off.[27]

There are different design procedures that can be followed when designing a broadband filter and a narrowband bandpass lumped element filter. Both design methods make use of immittance inverters and the mathematical models describing them. The impedance inverter can be defined by its ABCD matrix.

5.2: Immittance inverters

Immittance inverters and their mathematical properties are used when designing microstrip bandpass filters. The inverter is terminated with a load impedance or admittance, and the input of the inverter can be calculated by the following formula. The admittance inverter, also known as the J-inverter is a component with two ports on either side that produces the inverse of the load admittance connected. With one port of the J-inverter terminated by the load admittance Y_L , the input admittance Y_{in} can be calculated by using the following formula.

$$Y_{in} = \frac{J^2}{Y_L} \quad (15)$$

If the load admittance is capacitive or inductive, then the input admittance Y_{in} will become oppositely inductive or capacitive. This results in the inverter having a phase shift of off multiples of $\frac{\pi}{2}$. The ABCD matrix of an idea J-inverter is given by the following matrix.

$$\begin{bmatrix} A & B \\ C & D \end{bmatrix} = \begin{bmatrix} 0 & \pm \frac{1}{jJ} \\ \mp jJ & 0 \end{bmatrix} \quad (16)$$

5.3.1: Microstrip Bandpass Filter Design Procedure

The design process of the bandpass lumped element filter uses the formulae shown on the right. First the filter order or the number of resonators (n), is approximated. The ripple level is a known value given in the spec and is used to find

the lookup table that provides the g_i parameters for the appropriate filter order. These g_i parameters are used to calculate the admittance, susceptance, and capacitance of components in the equivalent circuit model as well as the electrical length and physical lengths of the resonators.

$$\gamma = \frac{f_s - f_0}{f_H - f_0} = \frac{4 - 3.5}{3.6 - 3.5} = 5 \quad (17)$$

$$n \geq \frac{6 + L_{IS} + L_R}{20 \log(\gamma + \sqrt{\gamma^2 - 1})} \geq \frac{6 + 25 + 15}{20 \log(5 + \sqrt{5^2 - 1})} \geq 2.81 \approx 3 \quad (18)$$

With the approximated filter order determined to be 3, the microstrip bandpass filter can be modelled as an equivalent J-admittance inverter circuit. Taking the ripple level from the filter specification as 0.1 dB, the g parameters are found using the appropriate lookup table and the obtained number of resonators, n . Using the g parameters taken across the row where $n = 3$ considering that $g_0 = 1$. The rest of the calculations take some time and repetition but eventually result in an initial filter design.

n	g_1	g_2	g_3	g_4	g_5	g_6	g_7	g_8	g_9	g_{10}
1	0.3052	1								
2	0.8431	0.6220	1.3554							
3	1.0316	1.1474	1.0316	1						
4	1.1088	1.3062	1.7704	0.8181	1.3554					
5	1.1468	1.3712	1.9750	1.3712	1.1468	1				
6	1.1681	1.4040	2.0562	1.5171	1.9029	0.8618	1.3554			
7	1.1812	1.4228	2.0967	1.5734	2.0967	1.4228	1.1812	1		
8	1.1898	1.4346	2.1199	1.6010	2.1700	1.5641	1.9445	0.8778	1.3554	
9	1.1957	1.4426	2.1346	1.6167	2.2054	1.6167	2.1346	1.4426	1.1957	1

Table II: Tables of g -parameters for the Chebyshev filter with ripple level 0.1 dB.

The admittance inverter values can be calculated with separate formulas for the beginning, intermediate and final edge structures. The value of δ must be determined, with the formula (19) where f_0 is the centre frequency 3.5 GHz. The frequencies f_1 and f_2 are the lower and upper bounds of the passband respectively and BW is the bandwidth 200 MHz. Where $f_1 = f_0 - \frac{BW}{2} = 3.4 \text{ GHz}$ and $f_2 = f_0 + \frac{BW}{2} = 3.6 \text{ GHz}$. Using the calculated admittances, the susceptance values are evaluated at the centre frequency f_0 .

$$\delta = \frac{f_1 - f_2}{f_0} = \frac{2}{35} \approx 0.0571 \quad (19)$$

$$\frac{J_{0,1}}{Y_0} = \frac{J_{3,4}}{Y_0} = \sqrt{\frac{\pi\delta}{2g_0g_1}} = \sqrt{\frac{\pi\delta}{2g_3g_4}} = \sqrt{\frac{\frac{2}{35}\pi}{2 \times 1.0316 \times 1}} = 294.975 \text{ mS} \quad (20)$$

$$\frac{J_{1,2}}{Y_0} = \frac{J_{2,3}}{Y_0} = \frac{\pi\delta}{2\sqrt{g_1g_2}} = \frac{\pi\delta}{2\sqrt{g_2g_3}} = \frac{\frac{2}{35}\pi}{2\sqrt{1.0316 \times 1.1474}} = 82.503 \text{ mS} \quad (21)$$

$$B_{i,i+1} = \frac{J_{i,i+1}}{1 - \left(\frac{J_{i,i+1}}{Y_0}\right)^2} \quad (22)$$

$$B_{0,1} = B_{3,4} = \frac{294.975 \times 10^{-3}}{1 - (294.975 \times 10^{-3})^2} = 323.087 \text{ mS}$$

$$B_{1,2} = B_{2,3} = \frac{82.503 \times 10^{-3}}{1 - (82.503 \times 10^{-3})^2} = 83.068 \text{ mS}$$

To calculate the physical lengths of the microstrip resonators, first the electrical lengths θ_i are calculated with the following formula.

$$\theta_i = \pi - \frac{1}{2} \left[\text{Arctan} \left(2 \frac{B_{i-1,i}}{Y_0} \right) + \text{Arctan} \left(\frac{B_{i,i+1}}{Y_0} \right) \right] \quad (23)$$

$$\theta_1 = \pi - \frac{1}{2} [\text{Arctan}(2 \times 323.087 \times 10^{-3}) + \text{Arctan}(83.068 \times 10^{-3})] = 2.81 \text{ rad}$$

$$\theta_2 = \pi - \frac{1}{2} [\text{Arctan}(2 \times 83.068 \times 10^{-3}) + \text{Arctan}(83.068 \times 10^{-3})] = 3.018 \text{ rad}$$

$$\theta_3 = \pi - \frac{1}{2} [\text{Arctan}(2 \times 83.068 \times 10^{-3}) + \text{Arctan}(323.087 \times 10^{-3})] = 2.903 \text{ rad}$$

With the calculated susceptance $B_{i,i+1}$, the series capacitances across the gaps between the microstrip lines can be approximated with the following formula. Where ω_0 is the angular frequency $2\pi f_0 = 21.99 \times 10^9 \text{ rad/s}$.

$$C_{i,i+1} = \frac{B_{i,i+1}}{\omega_0} \quad (24)$$

$$C_{0,1} = C_{3,4} = \frac{323.087 \times 10^{-3}}{2\pi \times 3.5 \times 10^9} = 14.69 \text{ pF}$$

$$C_{1,2} = C_{2,3} = \frac{83.068 \times 10^{-3}}{2\pi \times 3.5 \times 10^9} = 3.78 \text{ pF}$$

The physical lengths of the resonators l_i can be approximated with the following formula, the electrical lengths are divided by β to obtain the physical length of each resonator. Where $\lambda_g = 58.427 \text{ mm}$ from formula (14).

$$\beta = \frac{2\pi}{\lambda_g} = \frac{2\pi}{58.427 \times 10^{-3}} = 107.539 \quad (25)$$

$$l_i = \frac{\theta_i}{\beta} \quad (26)$$

$$l_1 = \frac{2.81}{107.539} = 26.13 \text{ mm}$$

$$l_2 = \frac{3.018}{107.539} = 28.06 \text{ mm}$$

$$l_3 = \frac{2.903}{107.539} = 26.99 \text{ mm}$$

The result of these calculations should provide a relatively accurate model that can be simulated and adjusted to match its behaviour to the specifications. The schematic diagram constructed in ADS is shown below in figure D. All microstrip line components in the circuit share the same substrate and width property, with the outer microstrip lines TL5 and TL4 having the same length of 10mm due to this length not having much effect on the impedance of the line. The resonators TL1, TL2 and TL3 have the physical lengths as determined in the previous calculations for l_1 , l_2 and l_3 . The distance across microstrip gaps is represented by the variable S on the MGAP components. As can be observed by the values obtained for the gap capacitances, the outer two gaps have a greater capacitance than that of the inner two. A greater gap capacitance must mean that gaps between microstrip line resonators are proportionally shorter in the distance.

To obtain reliable gap distances that can provide a capacitance comparable to the values calculates previously using the formula (24), there are several approaches that can be taken. To properly understand how the distance of the gap compares to the capacitance across it, each component can be isolated in separate ADS circuit schematics. The capacitor and the MGAP component can both be connected between two port terminations that have an impedance of 50 ohms and their negative terminals grounded. Both schematics are simulated with the same simulation parameters, and the MGAP component requires an MSUB component to define the substrate properties. The values set in the S-Parameters and MSUB components are the same as those used in previous simulations. The reason for the impedance of 50 ohms at each port termination is due the width of the microstrip lines across the filter staying consistent at 1.55mm which results in the microstrip lines having a characteristic impedance of 50 ohms regardless of their differing lengths.

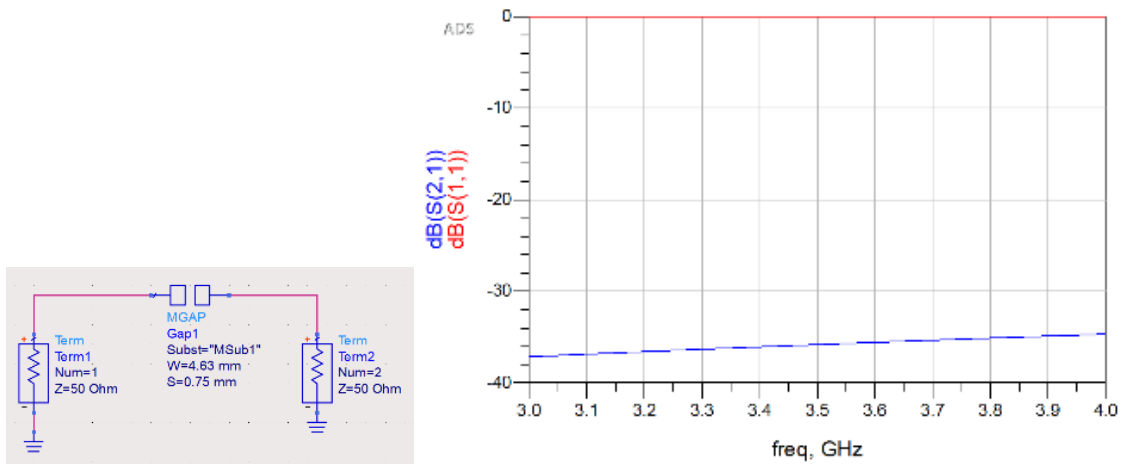


Figure 20: MGAP component circuit shown with simulation results showing reflection and transmission losses over a range of frequencies.

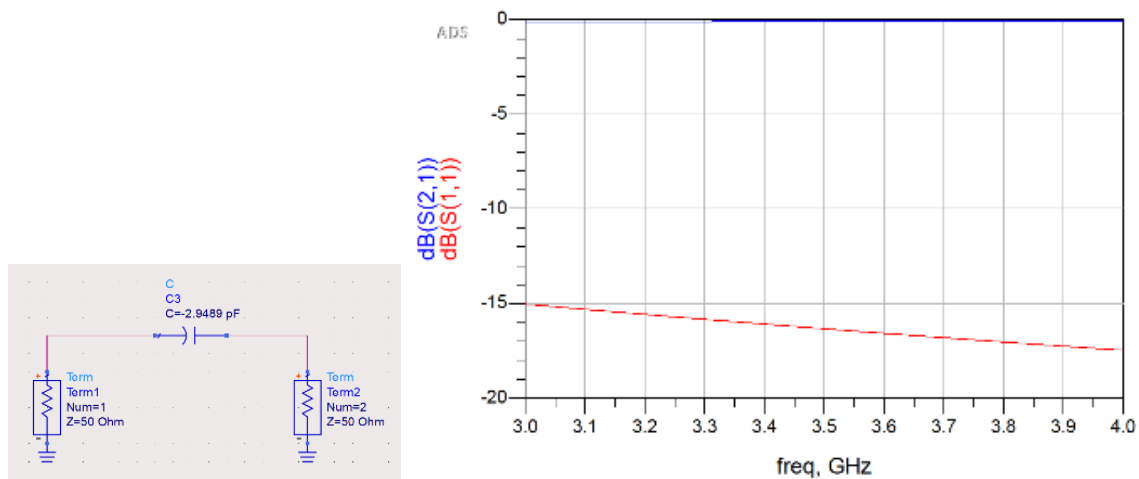


Figure 21: Basic capacitor component circuit shown with simulation results showing reflection and transmission losses over a range of frequencies.

The isolated component circuits are shown on the left with the results of their simulations shown on the right. A systematic approach is taken to trying to match the reflection and transmission loss response of the gap to that of the capacitor. The value of S is adjusted, simulated and the results are recorded and compared to the simulation results for the known capacitor. A conclusion drawn from these tests is that the behaviours of a capacitor compared to a microstrip gap is very different, and even though it may be useful in modelling an entire bandpass filter, alone they do not act as capacitors as much as expected.

A microstrip gap can be represented by an equivalent circuit. The shunt and series capacitances, C_g and C_p , can be determined by making use of some formulas derived from the transmission line model as can be seen in figure 5 d). However, upon performing these calculations, it becomes clear that these expressions will not apply in this case due to the expressions not being accurate outside a certain range for the width to height ratio and the dielectric substrate constant also being out of range.

Initially placeholder values are entered to the gap widths, these gap distances required much trial and error to optimise and were achieved by recalculating, rebuilding, and re-simulating.

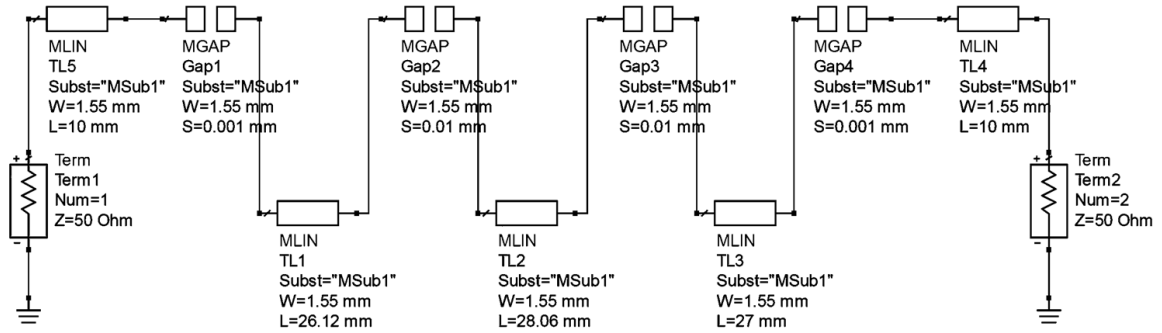


Figure 22: Circuit schematic of the microstrip bandpass filter.

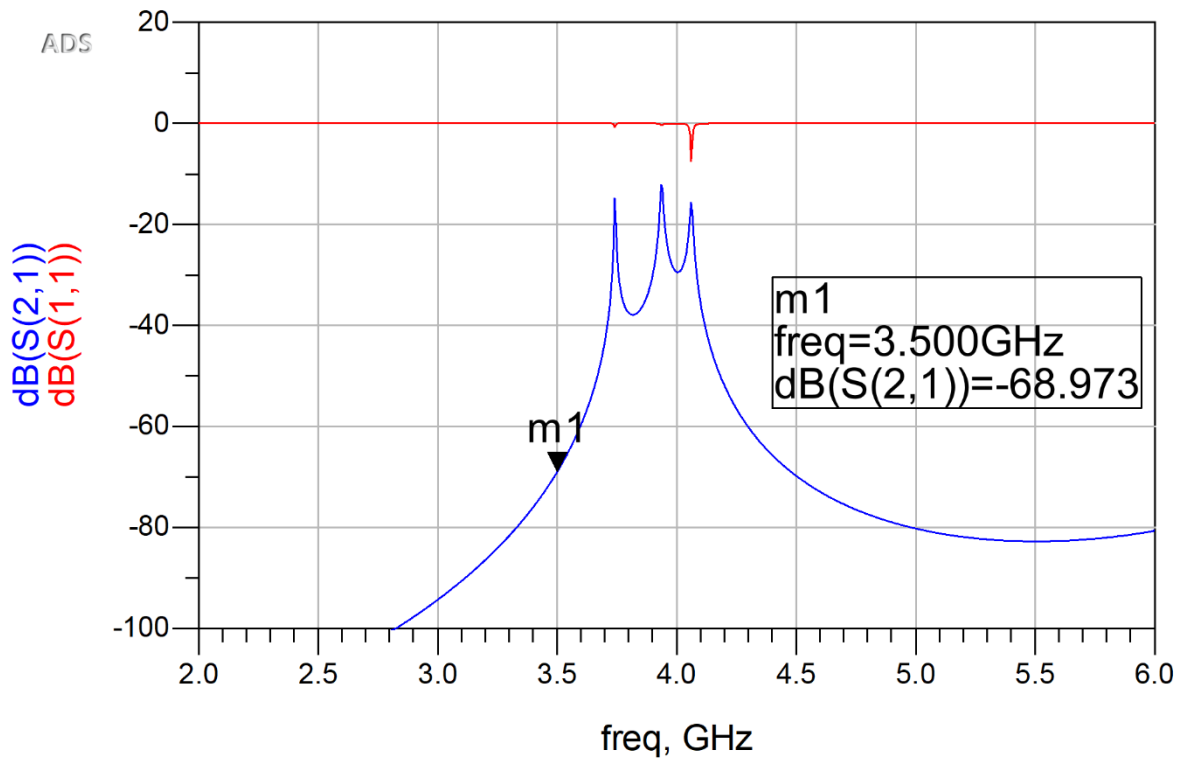


Figure 23: Microstrip bandpass filter simulation results showing reflection and transmission losses over a range of frequencies.

The resulting plot in figure 23 shows the reflection and transmission loss plotted over a short range of frequencies. At the specified resonant frequency, the transmission loss is observed to reach -68.97 decibels, this initial filter design gives us an inaccurate result and must be tuned to provide a lower minimum reflection loss at the desired resonant frequency. The reflection and transmission loss appear to have an inversely proportional relationship, with the transmission loss increasing as the reflection decreases. When transmission loss is at minimum, reflection loss does not differ much from its maximum value of 0 decibels.

5.3.2: Optimisation

As the simulation results of the initial filter design were inaccurate, certain values can be adjusted within range, to tune the filter to behave more accurately to

the specification. The circuit schematic shown below in figure 24 shows the optimised circuit diagram, that is supposed to provide a more accurate response.

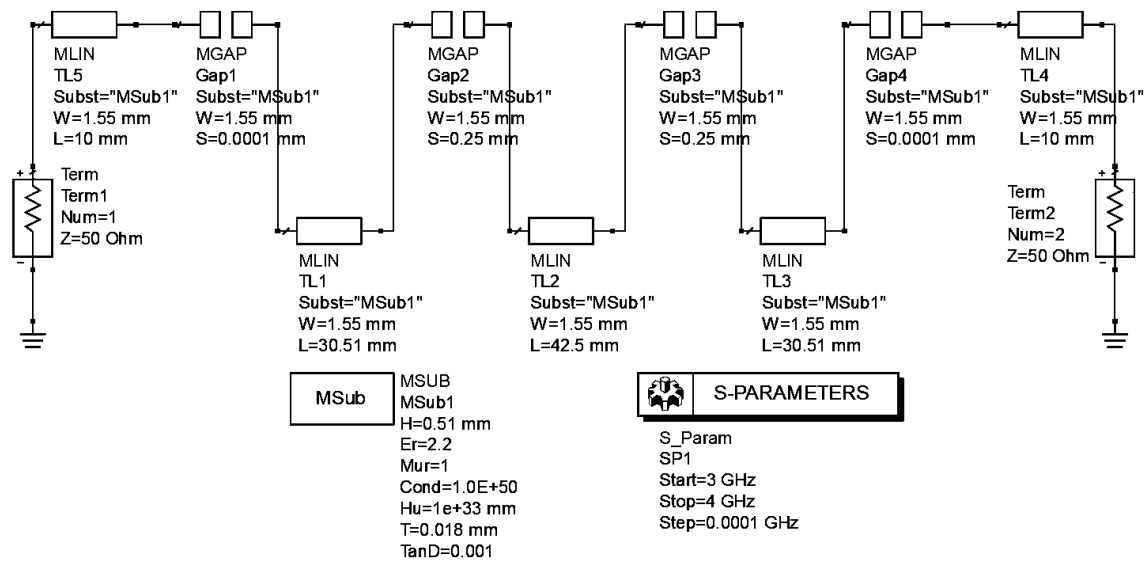


Figure 24: Circuit schematic of the optimised microstrip bandpass filter.

The optimised values for gap distances (S) and resonator lengths (W), have been determined iteratively through re-simulation, trial and error and averaging the difference. Using these values, the microstrip bandpass filter is simulated and the transmission and reflection loss in dB is measured to behave accurate to the desired specification.

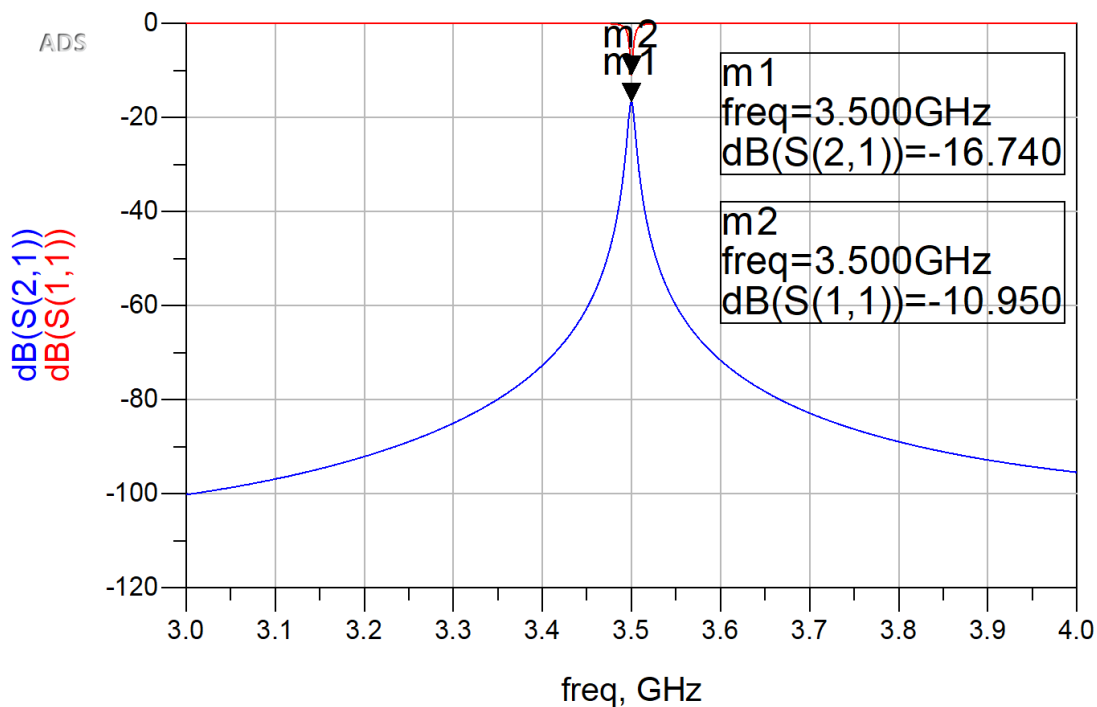


Figure 25: Microstrip bandpass filter simulation results showing reflection and transmission losses over a range of frequencies.

The optimised microstrip bandpass filter now provides a reflection loss of -16.74 dB at the resonant frequency, which means that about 2% of the received energy is lost due to it being reflected away. The transmission loss is simulated to be a -10.95 dB at 3.5 GHz, which is about 8% of the energy being lost due to transmission. The optimised filter response manages to stay well within the limits outlined in the specification with great accuracy, the return loss within the passband is much lesser than 15 dB, and the insertion loss is much less than 2 dB. The results fulfil the specification however the filter component could be tuned no further due to the ongoing COVID-19 situation. Which has caused a reduced availability in crucial software licenses and equipment used generate a layout and further simulate and analyse the characteristics.

The overall physical dimensions of the designed filter component is approximately 124.02mm in length and 1.55mm in width with a height of 1.6mm

5.4: Filtenna

The overall design of this wireless energy harvesting microstrip filtenna is broken down into two constituent components, the rectangular patch array, and the bandpass filter. Both are designed to be fabricated with the available resources and within limitations, making use of microstrip line technology. The WEH system must be able to convert the desired radio frequency signals in the surrounding environment into a stable energy source that is sufficient to power something like the sensor unit described in the introduction and shown in Figure 1. Considering that the target environment for this technology is likely to have an abundance of these mid-band 5G signals, the WEH filtenna must be designed to be integrated into an Internet of Things network that is communicating via 5G at a frequency range that is less than 6GHz.

The design of all the constituent components have been simulated, tested, and tuned to the specification. The overall filtenna device can now be finalized in a circuit schematic by combining the antenna to the bandpass filter directly. First, the filter is connected to a single antenna element and simulated, this demonstrates the effect that increasing the number of antennas has on the loss response of the filtenna.

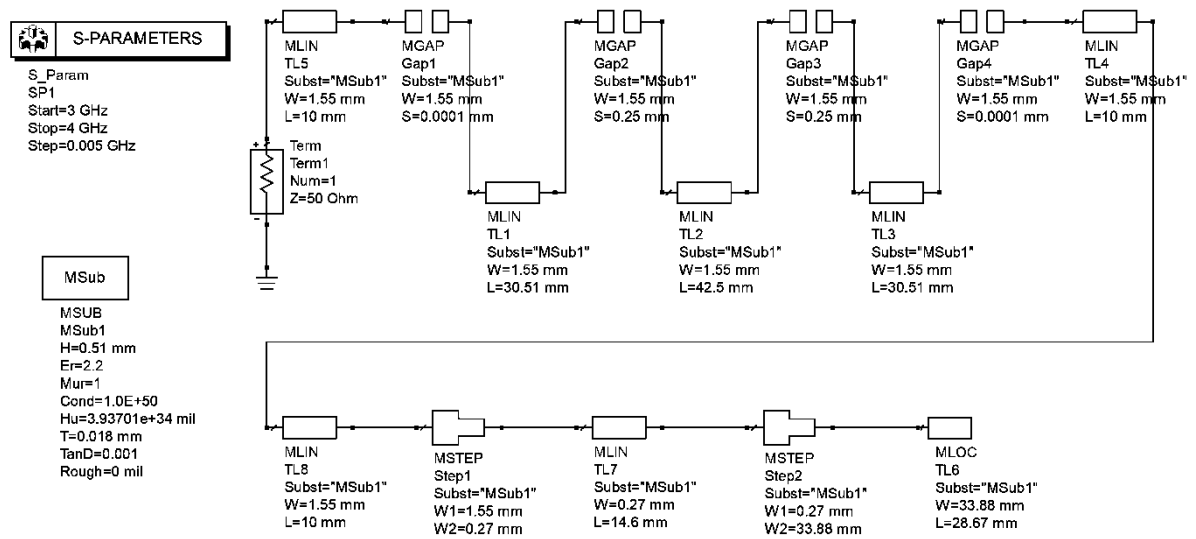


Figure 26: Complete filtenna circuit schematic.

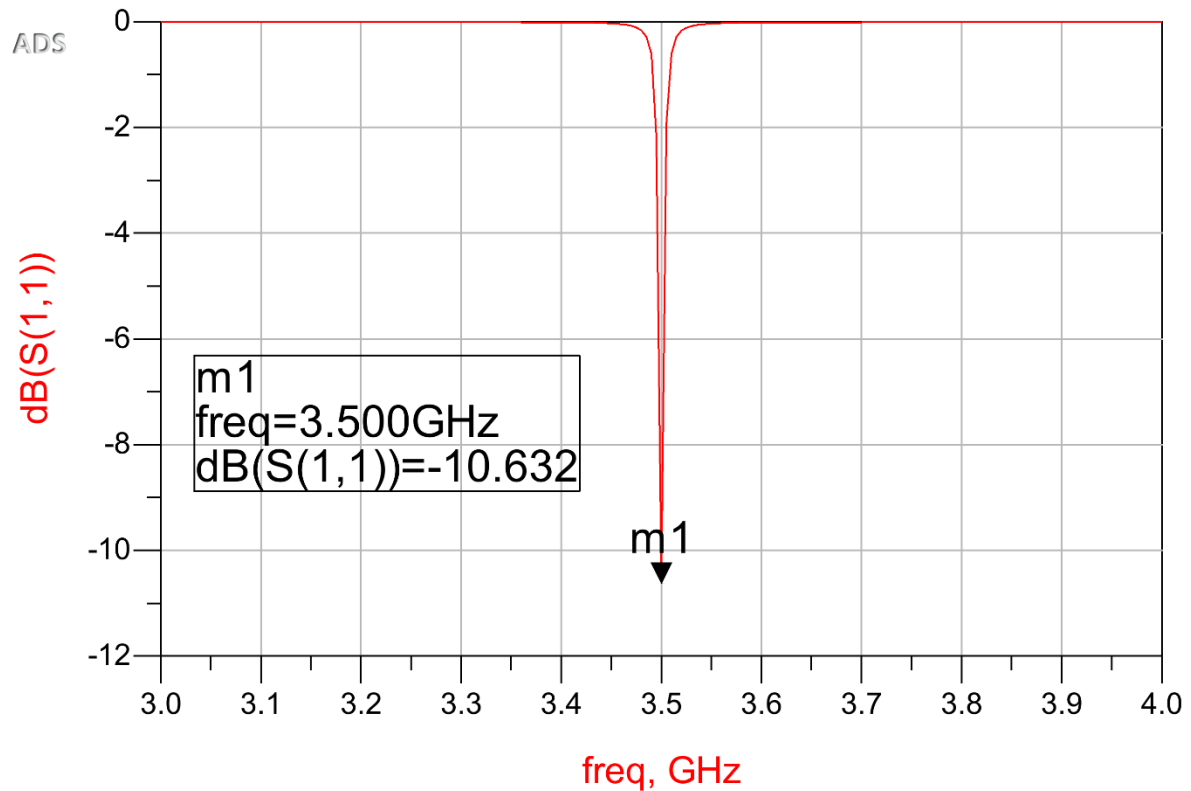


Figure 27: Graph showing simulation results for filtenna with single antenna element.

There is no transmission loss only reflection loss, this is due to the filtenna circuit terminating with a MLOC component that represents the rectangular patch. This graph shows reflection loss over range of frequencies with a marker m1 placed at the desired resonant frequency. At 3.5 GHz the initial filtenna design can be expected to provide a loss of -10.632 decibels meaning that only about 8.6% of the energy that this filtenna device receives would be lost due to reflection. The result is satisfying and well within the specifications for the project design.

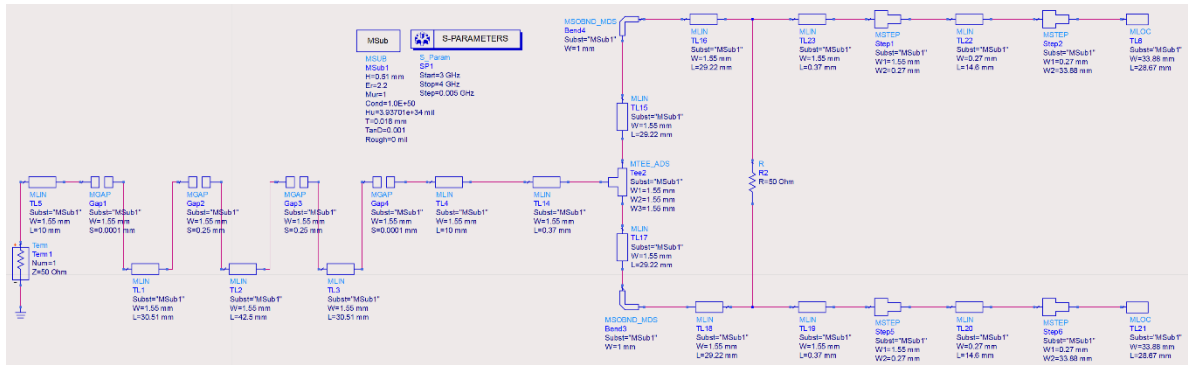


Figure 28: Complete Filtenna circuit schematic with a 1x2 antenna array.

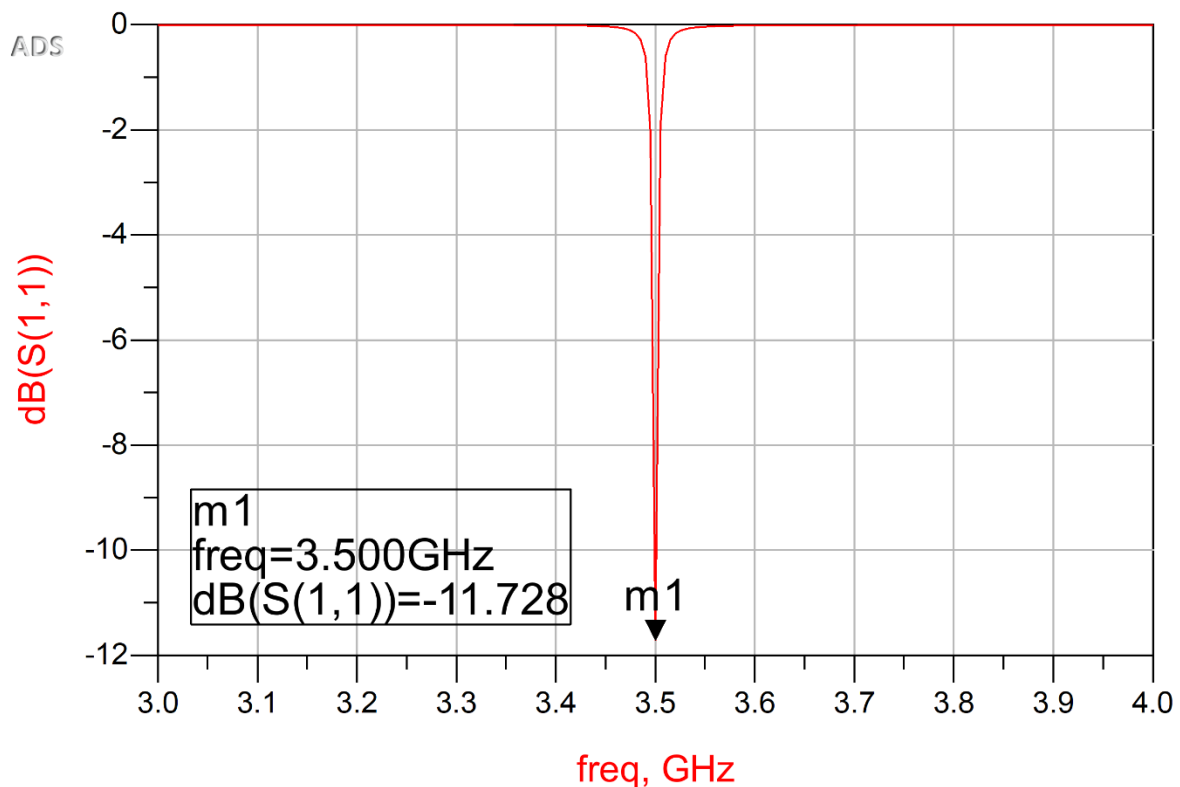


Figure 29: Microstrip filtenna with 1x2 array simulation results.

The simulation results for the filtenna component with the 1x2 antenna array show that at the resonant frequency, the reflection loss is -11.728 decibels. This means that about 6.7% of the energy that the microstrip filtenna receives is lost due to reflection. Increasing the amount of antennas connected to the bandpass filter has decreased the reflection loss by about 1.1 decibels.

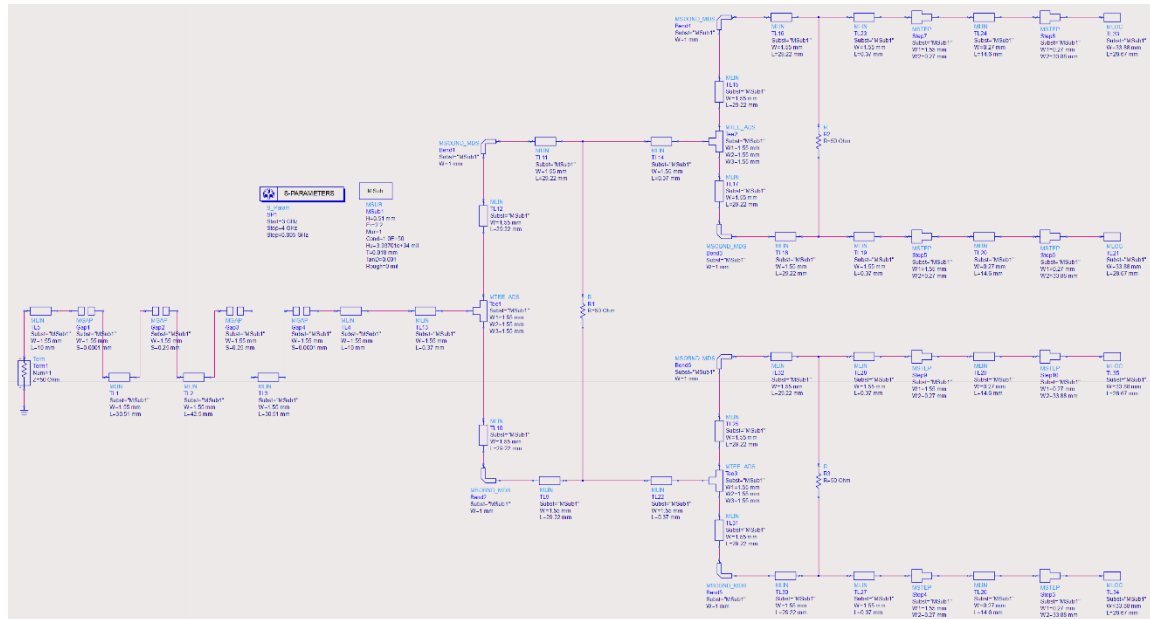


Figure 30: Complete Filtenna circuit schematic with 1x4 antenna array.

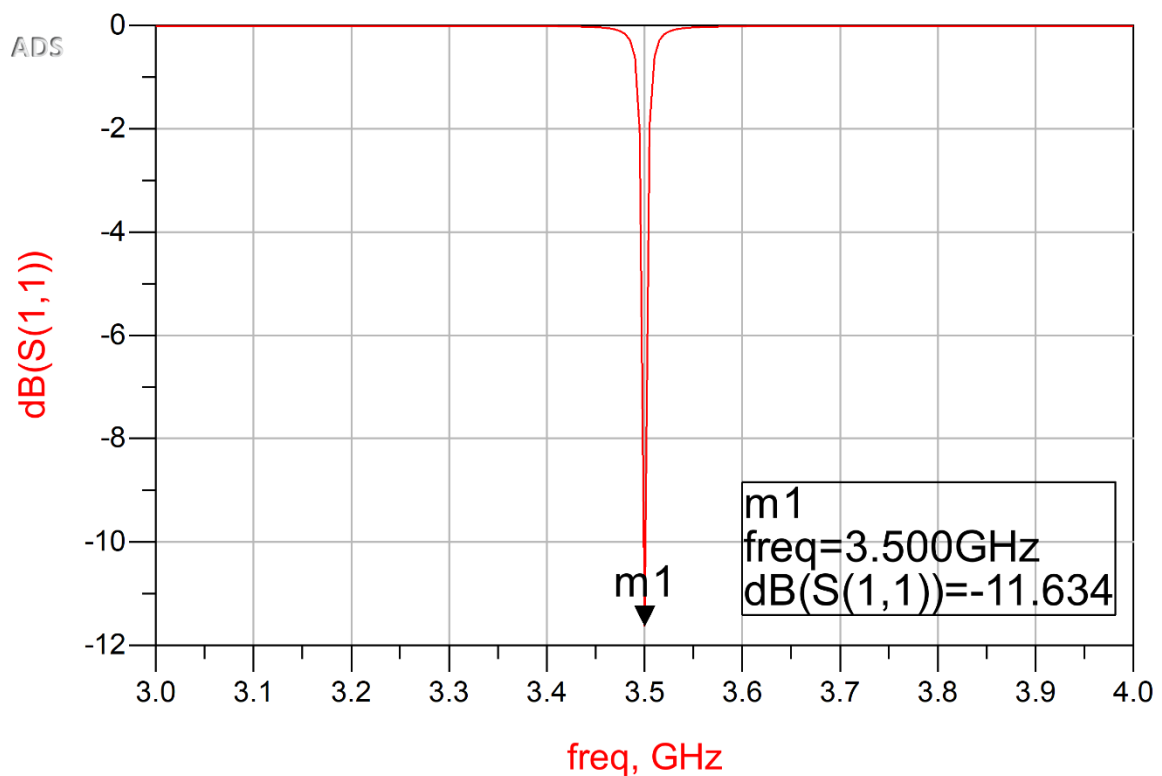


Figure 31: Microstrip filtenna simulation results showing reflection loss over a range of frequencies.

The final filtenna design with a 1x4 antenna array connected to the microstrip bandpass filter is simulated in ADS to provide the graph shown above in figure 27. At the centre frequency of 3.5 GHz, the reflection loss is -11.634 dB which means that about 6.9% of the energy that is received by the 1x4 patch antenna array is lost due to reflections throughout the microstrip filtenna structure. While this is still well within the specifications, this amount of loss at the resonant frequency is slightly more than is provided with the 1x2 array. However the increased number of

antenna elements does increase the downlink/uplink capacity and received power gain of a MIMO system, as described in chapter 2.1.

Chapter 6: Resources

The resources that have been used to carry out the work done on this project have been made available by the university to the of the best of their ability under the current circumstances. Making use of several software licenses, for software tools including Advanced Design System (ADS), MATLAB and of course Microsoft office. The software called EmSonnet, that is mainly used for electromagnetic simulation was not available to be licensed for academic use for the purposes of this project and therefore this paper does not spend too much time discussing the electromagnetic field behaviour or the fabrication of the designed components.

Chapter 7: Project Specification

The specifications that were decided upon for the design is influenced by previous work that has been done on the subject, as well as the resources available for both design and fabrication. Values are taken from the specification and included in calculations and model simulations that are taken in the design section.

Patch antenna specification:

- Centre frequency: 3.5 GHz
- Bandwidth: 200 MHz
- Reflection coefficient (S_{11}): > -15 dB
- Source impedance (Z_0): 50Ω
- Conducting Layer thickness (t):
0.018mm
- Conductor Material: Cu 337
- Substrate Material: Composite micro
-fibre glass
- Dielectric Constant (ϵ_r): 2.2
- Substrate Thickness (h): 0.510mm
- Overall High of substrate (H): 1.6mm

Filter Specification:

- Centre frequency: 3.5 GHz
- Bandwidth: 200 MHz
- Ripple Level: 0.1 dB
- Passband Return Loss: > 15 dB
- Passband Insertion Loss: < 2 dB
- Rejection @ 4GHz: 35 dB
- Source and Load Impedance: 50Ω
- Filter Type: Chebyshev

Chapter 8: Ethical and environmental issues

There are several issues that can be raised concerning the ethical and environmental repercussions that this project could have. These relate to high frequency radio wave exposure to health and safety issues regarding construction and using heavy machinery.

8.1: 5G panic

Many people have concerns over the risks to being exposed to 5G, however these are mostly unwarranted. The levels of RF radiation emitted from base stations and mobile phones adheres to the international health and safety regulations [10]. Maintaining levels of exposure hundreds of times below the guideline limits in public areas.

8.2: The ethical and environmental issues of MIC technology

The apparatus used in the fabrication of the microstrip components pose a risk to the user's health and safety because machinery such as a circuit board plotter have very sharp blades used for cutting out the microstrip components into shape. Standard health and safety measure apply when using such equipment as to decrease the potential risk to the individual's health and safety.

- Eye protection must be always worn, including PPE when working in the labs during the pandemic.
- Long hair must be tied back.
- Safety boots with hard toe caps must be worn.
- Ties or any loose clothing that could hang and get stuck in the moving parts of the machine must be tucked in.
- An emergency stop button must be functional and within reach of the apparatus.

Environmental issues with MIC components are mostly attributed to the way in which they are disposed of. The substrate material is micro-fibre glass which is non-biodegradable and takes a high amount of energy to produce compared to natural fibres. This results in a contribution to landfills worldwide as broken circuits that are not properly recycled and contributes to the release more CO₂ into the atmosphere from the energy required to produce the glass. A compromise could be met somewhere, where circuits are recycled effectively, and less energy is spent fabricating new micro-fibre glass. The conducting material is copper which can be recycled and repurposed with ease.

Chapter 9: Conclusion

9.1: Summary

The primary objective for this project was to design a wireless energy harvesting filtenna that operates at 3.5 GHz and can be integrated into an internet of things network to improve the energy efficiency of interconnected devices. This goal has been met, with the resulting component design receiving the desired sub-6 GHz 5G signals and effectively filtering out the other frequencies outside of a 200 MHz bandwidth. To further improve upon these results, much more time is to be dedicated to optimising the gap distances and resonator lengths to provide the ideal response with the smallest possible loss in the passband. With the circumstances around national lockdown measures in place, it was not possible to conduct some electromagnetic simulations of the microstrip components due to the software license for the program EmSonnet unfortunately not being available for use. The construction of the filtenna component would make use of a ProtoMat C60 circuit board plotter and testing would make use of various measuring equipment such as a Vector Network Analyzer which would be used to evaluate the performance and behaviour of the designed components.

In the introduction and chapter 2, wireless energy harvesting sub-systems for 5G internet of things were explored as a solution to supporting the energy costs of this modern infrastructure of 5G smart devices. In chapter 4, the microstrip patch antenna and antenna arrays were described, designed, and simulated in ADS. Electromagnetic simulations and fabrication of these antenna components were not possible to carry out due to the reasons previously elaborated on. Despite these obstacles, the designed components were tuned to provide an optimal response sufficiently accurate to the one defined in the specification. In chapter 5, the microstrip lumped element parallel coupled bandpass filter was described, designed, simulated and then iteratively optimised to provide a behaviour sufficiently accurate to the one defined in the specification. The choices made for the filtenna design are justified in the research. The rectangular patch antenna is relatively light weight and structurally compact in comparison to other kinds of RF antennas. The fabrication process is low cost and simple, making use of equipment that are already used in PCB manufacture. Microstrip end-coupled bandpass filters provide the advantage of high rejection roll off and are the optimal choice for applications with narrow bandwidth such as this.

There is further work that can be done on this project to fully prepare the filtenna component to be integrated into an Internet of Things network. The objectives concerning electromagnetic simulation, implementation, building and testing of the designed components could not be met due to the university being closed due to COVID-19 pandemic. It would have been beneficial to be able to fabricate each of the microstrip patch antenna arrays to analyse them and test them in the lab with the proper equipment. A WEH device for IoT can convert alternating RF currents into a DC power source which could be stored in an on-board power storage component

such as a capacitor, or the DC voltage produced could be used to bias something like an amplifier. With increased time and resources, it would be interesting to investigate the results of rectifying the received and filtered signals. This would be done by connecting a rectifier to the matching filtenna circuit, which would convert the received RF energy into DC power source. In chapter 5 section 4, the filtenna design comes together combining the microstrip antenna components with the bandpass filter to achieve a reflection loss of about 7% at the desired resonant frequency of 3.5 GHz. The bandwidth observed in the simulation results was narrower than the specified 200 MHz, however this could be overcome with some trial and error. Increasing the number of antennas on the receiving antenna array will also increase the received power gain. Therefore the final filtenna design, using the 1x4 antenna array, is the product of this project, sufficiently serving the desired purpose within the set specifications.

Work Plan

	Sep	Oct	Nov	Dec	Jan	Feb	Mar	Apr
MIC Research								
5G IoT WEH Research								
Antenna Research								
Filter Research								
Learn ADS								
Learn EM Sonnet								
Design and Implementation								
Testing and Tuning								
Poster Presentation								
Report Writing								

Figure 32: Project Workplan

References

1. D. Budimir, "RF and Microwave Antenna for Communication Systems", September 2020.
2. Sonnet Software Inc. USA, "Sonnet 14.53 Lite Plus User Guide", March 2007.
3. K. Gupta, N. Sahayam, "A Review on Microstrip Filter for the Application in Communication System", International Research Journal of Engineering and Technology (IRJET), December 2018.
4. C. J. Kikkert, "A Design Technique for Microstrip Filters", in 2nd International Conference on Signal Processing and Communication Systems, Gold Coast, December 2008.
5. BBC, "Click: Is 5G safe?", from TV programme Click, November 2019.
6. P. Kamalinejad, C. Mahapatra, Z. Sheng, S. Mirabbasi, V. C. M. Leung and Y. L. Guan, "Wireless energy harvesting for the Internet of Things," in IEEE Communications Magazine, vol. 53, no. 6, June 2015.
7. S. Symanovich, "The future of IoT: 10 predictions about the Internet of Things," in NortonLifeLock, August 2019.
8. Sagentia, "Energy Harvesting", in A Sagentia white paper, Dec 2014.
9. B. Haney, "Is microfiber green? Comparing microfiber's environmental impact with cotton and paper", Microfiber Wholesale, January 2020.
10. NHS Department of Health and Social Care, "Mobile phones and base stations", in government leaflet, February 2011.
11. T. J. Kazmierski, S. Beeby, "Energy Harvesting Systems: Principles, Modeling and Applications", 2011.
12. Hendricks, Drew. "The Trouble with the Internet of Things". London Datastore. Greater London Authority. Retrieved 10 August 2015.
13. Keysight Technologies, "Advanced Design System (ADS) 2017 Documentation", 2017.
14. D. D. Grieg and H. F. Engelmann, "Microstrip-A New Transmission Technique for the Kilomegacycle Range," in Proceedings of the IRE, vol. 40, no. 12, pp. 1644-1650, Dec. 1952
15. C.A. Balanis, "Antenna Theory: Analysis and Design," John Wiley & Sons, Inc., New Delhi, 2005.
16. Horwitz, Jeremy (December 10, 2019). "The definitive guide to 5G low, mid, and high band speeds". VentureBeat online magazine. Retrieved April 23, 2020.
17. Tesla, Nikola (June 1900). "The Problem of Increasing Human Energy". Century Magazine. Retrieved 20 November 2014.
18. Cory, H. (January 1981). "Dispersion characteristics of microstrip lines". IEEE Transactions on Microwave Theory and Techniques. MTT-29: 59-61.
19. Madhav, B. & Rao, Tumati & Tirunagari, Anilkumar. (2018). Design of 4-element printed array antenna for ultra-wideband applications. International Journal of Microwave and Optical Technology. 13. 8-17.

20. Howard, Philip N. (2015). Pax Technica: How the internet of things May Set Us Free, Or Lock Us Up. New Haven, CT: Yale University Press. ISBN 978-0-30019-947-5.
21. Sanchez-Barberty, Mauricio, Design and implementation of a transceiver and a microstrip corporate feed for solid state x-band radar, 2021
22. Microwaves 101, Wilkinson Power Splitters, 22 April 2021
23. Prakash Moorut, 5G at 3.5 GHz: The Global Opportunity, 29 October 2019.
24. Ali A. Zaidu, Robert B. et al, Waveform and Numerology to Support 5G Services and Requirements, Ericsson Research Sweden, 2017.
25. "Enabling 5G in the UK", Ofcom.org.uk, 2018.
26. Dr. D. Budimir, "MIMO Antenna Systems", September 2020.
27. Dr. D. Budimir, "Filter Technologies", September 2020.